hydrology

MDPI

Article

Streamflow Modeling of the Tulijá River Basin, Mexico, Using Near-Real-Time Satellite Precipitation Products

Lorenza Ceferino-Hernández [1,*], Khalidou M. Bâ [1], Francisco Magaña-Hernández [2], Miguel A. Gómez-Albores [1], Guillermo Pedro Morales-Reyes [1], Carlos Alberto Mastachi-Loza [1] and Carlos E. Torres-Aguilar [2]

[1] Instituto Interamericano de Tecnología y Ciencias del Agua, Universidad Autónoma del Estado de México, km 14.5 Carretera Toluca-Ixtlahuaca, Toluca 50200, Mexico; khalidou@uaemex.mx (K.M.B.); magomeza@uaemex.mx (M.A.G.-A.); gpmoralesr@uaemex.mx (G.P.M.-R.); camastachil@uaemex.mx (C.A.M.-L.)

[2] División Académica de Ingeniería y Arquitectura (DAIA), Universidad Juárez Autónoma de Tabasco, Carretera Cunduacán-Jalpa de Méndez km. 1, Cunduacán 86690, Mexico; francisco.magana@ujat.mx (F.M.-H.); enrique.torres@ujat.mx (C.E.T.-A.)

* Correspondence: lceferinoh001@alumno.uaemex.mx

Abstract

The use of remote sensing data in hydrological applications has increased, especially in regions with limited ground-based observations. Satellite precipitation products (SPPs) provide extensive temporal and spatial coverage but may contain biases that can affect their performance in hydrological simulations. This study evaluates the performance of four near-real-time SPPs for daily streamflow modeling in the Tulijá River Basin (TRB), Mexico: Precipitation Estimation from Remotely Sensed Information using Artificial Neural Networks (PERSIANN)-Cloud Classification System (CCS), PERSIANN-Dynamic Infrared Rain Rate near real-time (PDIR-Now), and the Early Run and Late Run products of the Integrated Multi-satellitE Retrievals for Global Precipitation Measurement (GPM) (IMERG). The SPPs were first compared with meteorological station precipitation data and subsequently bias-corrected using the Linear Scaling (LS) method. The CEQUEAU hydrological model simulated streamflow using three precipitation datasets: meteorological stations, original SPPs, and bias-corrected SPPs. For simulations using observed precipitation, the model was calibrated for 1991–2014 and validated for 1968–1990; for SPP-based simulations, calibration and validation were performed for 2003–2011 and 2012–2014, respectively. Model performance was assessed using the Nash–Sutcliffe efficiency (NSE), percent bias (PBIAS), and coefficient of determination (R^2). The results show that CEQUEAU performance varies by precipitation dataset. Simulations using observed precipitation yielded NSE values close to 0.70 during both calibration and validation, whereas the original SPPs yielded NSE values below 0.18, including negative values. After bias correction, IMERG-Early and IMERG-Late yielded NSE values of approximately 0.55 during both periods. These findings highlight the importance of analyzing the performance of near-real-time SPPs in hydrological applications, especially in tropical regions with complex topography.

Keywords: bias correction; hydrological model; streamflow simulation; satellite precipitation; Tulijá River Basin

Check for updates

Academic Editor: Guoqiang Tang

Received: 10 July 2026
Revised: 27 August 2026
Accepted: 28 August 2026
Published: 30 August 2026

Copyright: © 2026 by the authors. Licensee MDPI, Basel, Switzerland. This article is an open access article distributed under the terms and conditions of the Creative Commons Attribution (CC BY) license.

1. Introduction

Precipitation is the most important input variable for hydrological modeling and hydrometeorological applications; therefore, reliable and accurate precipitation data are essential for flood and drought forecasting. However, in both developing and developed countries, the spatial distribution of ground-based precipitation measurement instruments (rain gauges and weather radars) is often inadequate, even though these instruments are considered the most reliable methods for measuring precipitation. This situation hinders water management and distribution in many regions and reduces the effectiveness of flood early warning systems, leading to significant socioeconomic impacts [1,2].

With the advent of meteorological satellites, several SPPs have been developed over the past few decades as an alternative source of precipitation information. These products are available with near-global coverage and at different temporal resolutions. Among the most widely used are the Climate Prediction Center (CPC) Morphing Technique (CMORPH) [3]; the Climate Hazards Group InfraRed Precipitation with Stations (CHIRPS) [4]; the NOAA Climate Prediction Center Rainfall Estimates (RFE) [5]; the Tropical Rainfall Measuring Mission (TRMM) [6]; the Global Satellite Mapping of Precipitation (GSMaP) [7]; the Precipitation Estimation from Remotely Sensed Information using Artificial Neural Networks (PERSIANN) [8]; and the Integrated Multi-satellite Retrievals for Global Precipitation Measurement (GPM) (IMERG) [9], among others. Each of these SPPs differs in the techniques used to estimate rainfall; therefore, their applicability to streamflow simulation needs to be evaluated across different regions.

Among the available SPPs, PERSIANN-CCS and PDIR-Now, in addition to providing near-real-time precipitation estimates, are characterized by their high spatial ($0.04^\circ \times 0.04^\circ$) and temporal resolution. Consequently, several studies have evaluated their performance in hydrological applications [10–15]. Gunathilake et al. [16] evaluated the performance of PERSIANN, PERSIANN-CCS, and PDIR-Now using the Hydrologic Engineering Center-Hydrologic Modeling System (HEC-HMS) model in the Seethawaka River Basin, Sri Lanka, during two extreme rainfall events that occurred in 2016 and 2017. They concluded that these products could not adequately reproduce peak streamflows. Similarly, Ndemere et al. [17] evaluated four SPPs, including PERSIANN-CCS and PDIR-Now, to simulate daily streamflow using the HEC-HMS model at three gauging stations in Zimbabwe's Eastern Highlands. The authors reported that PERSIANN-CCS and PDIR-Now underestimated streamflow.

Bertini et al. [18] used PERSIANN-CCS as input data for a model based on the Width Function Instantaneous Unit Hydrograph (WFIUH) to simulate streamflow in a basin in Italy over 2005–2015. The simulations assumed streamflow data were unavailable for model calibration to reproduce ungauged conditions. In addition, Eini et al. [19] analyzed the performance of different products from the PERSIANN family for hydrological simulation in the Wełna River Basin, Poland, using the Soil and Water Assessment Tool+ (SWAT+) eco-hydrological model at daily and seasonal scales. Cao et al. [20], meanwhile, used PDIR-Now, IMERG-Early, and IMERG-Late estimates to generate merged precipitation products through a multi-SPE framework based on Triple Collocation (TC), without using observed precipitation data. They subsequently evaluated the hydrological utility of these products under ungauged conditions using the Beijiang River Basin in southern China.

Near-real-time IMERG products have also been widely evaluated in hydrological applications due to their high spatial and temporal resolution and their availability across different latencies. Accordingly, several studies have analyzed their performance in different regions worldwide, including China [21,22], the United States [23], Morocco [24], the United Kingdom [25], Nepal [26], and Malaysia [27]. Li et al. [28] analyzed the hydrological utility of IMERG-Early, IMERG-Late, and IMERG-Final data in a basin in China using the

SWAT model. They found that IMERG-Final performed best in daily streamflow simulation, whereas the near-real-time versions showed greater limitations. Similarly, Yan et al. [29] evaluated IMERG-Early and IMERG-Final using the Dominant River Routing Integrated with VIC Environment (DRIVE) model. They observed that IMERG-Final performed better for streamflow simulation. These findings indicate that near-real-time versions still contain uncertainties that may affect their application in hydrological modeling.

A recent study by Pourentezari et al. [23] evaluated the performance of four near-real-time SPPs (PERSIANN-CCS, PDIR-Now, IMERG-Early, and IMERG-Late) in northern California for peak streamflow estimation and flood forecasting using the HEC-HMS model. In addition, they applied bias correction using Long Short-Term Memory (LSTM) networks with IMERG-Final data. They concluded that bias correction improved the quality of the precipitation input data, which resulted in more accurate streamflow simulations.

SPP estimates often exhibit biases; therefore, correcting them before use in hydrological applications is recommended. These biases mainly stem from discrepancies in precipitation event detection, errors in estimating rainfall intensity and spatial distribution, and limitations of satellite algorithms in adequately representing certain types of precipitation, such as short-duration convective storms and orographic rainfall.

To address this issue, several studies have proposed various statistical and empirical approaches to adjust satellite precipitation estimates and improve their consistency with observed records [30–35]. Linear Scaling (LS) is one of the most widely used methods for bias correction because of its low computational cost, ease of implementation, and strong performance across different regions [36–41]. LS adjusts satellite precipitation values using factors derived from observed data, thereby reducing systematic bias and improving their applicability to hydrological modeling. Soo et al. [42] investigated three bias-correction methods (LS, local intensity scaling, and power transformation) applied to four SPPs (IMERG, CMORPH, TRMM, and PERSIANN) over the Langat River Basin, Malaysia. They analyzed their performance during five extreme flood events that occurred in December and January between 2013 and 2017. Adem et al. [43] applied the LS method to bias-correct three SPPs: TRMM-3B42, TRMM Real-Time (TRMM-3B42RT), and CHIRPS, and analyzed their impact on runoff simulation in the Wadi Nu'man Basin, Saudi Arabia, over the 2006–2018 period using HEC-HMS. These studies show that LS provides a practical, reliable approach to reducing systematic bias in SPPs while remaining simple to implement.

Other recent studies have evaluated various statistical and machine-learning methods to reduce systematic errors in SPPs before using them as inputs to hydrological models [44–46]. Overall, these studies agree that bias correction improves precipitation representation and, consequently, increases the accuracy of hydrological simulations. Although numerous studies have evaluated the performance of near-real-time SPPs in different regions, uncertainties remain regarding their hydrological performance in tropical regions such as southeastern Mexico. Due to its geographical location, this region is frequently affected by hurricanes, tropical storms, and intense rainfall events, which pose significant challenges for SPPs. In this context, the present study had two main objectives: (i) to evaluate the performance of four near-real-time SPPs (IMERG-Early, IMERG-Late, PERSIANN-CCS, and PDIR-Now) for simulating daily streamflow in the TRB, Chiapas, Mexico, using the CEQUEAU hydrological model, and (ii) to assess the effect of the LS bias-correction method on the estimates from these products and the resulting improvement in streamflow simulations. The findings of this study are expected to improve understanding of the performance of these SPPs in complex tropical environments and to support flood monitoring and water resources management in the region.

2. Study Area, Dataset, and Hydrological Model

2.1. Study Area

The study area focuses on the Tulijá River Basin (TRB) up to the Salto de Agua hydrometric station. The basin is located in the state of Chiapas, Mexico, covering a drainage area of 3561 km^2, and extends between latitudes 16°45′ N and 17°48′ N and longitudes 91°27′ W and 92°30′ W (Figure 1). Elevation within the TRB ranges from 4 m to 2476 m above sea level (m a.s.l).

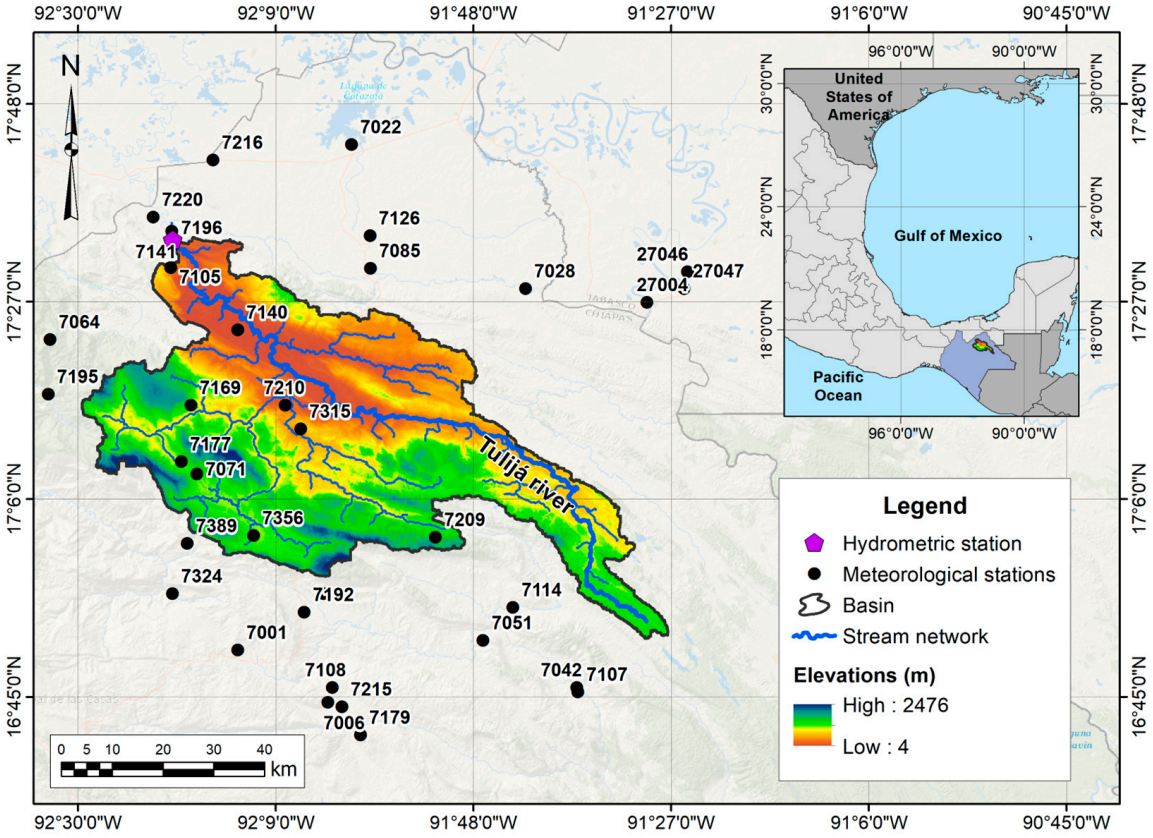


Figure 1. Study area: TRB, location of the hydrometric station, and meteorological stations used in the study.

Four climate types are present within the basin: humid tropical, semi-warm subhumid, semi-warm humid, and humid temperate, with the humid tropical climate predominating and rainfall occurring year-round. Mean annual precipitation is distributed within four ranges: 1500–2000 mm, 2000–2500 mm, 2500–4000 mm, and greater than 4000 mm, reflecting the variability in rainfall conditions across the TRB. The highest precipitation amounts are recorded in the northern part of the basin. The wettest months are September, October, and November, during which monthly rainfall can reach up to 800 mm. In contrast, the driest months are March and April, with monthly accumulations of approximately 100 mm.

Precipitation in the TRB is concentrated during the rainy season, when frequent flooding occurs. These floods not only affect the population within the basin but also contribute to flooding in the downstream Grijalva River, one of the most important river systems in southeastern Mexico. Therefore, the TRB is a suitable study area for hydrological modeling using near-real-time SPP estimates to improve flood management and monitoring in the region.

2.2. Dataset

2.2.1. Near-Real-Time Satellite Precipitation Products (SPPs)

The four near-real-time SPPs employed in this study estimate precipitation using different techniques and algorithms; consequently, they present different spatial and temporal resolutions, as summarized in Table 1.

Table 1. Characteristics of the four near-real-time SPPs employed in this study.

Name	Latency	Spatial Resolution	Temporal Resolution	Temporal Coverage	References
IMERG-Early	4 h	0.10° × 0.10°	Half-hourly	January 1998-present	Huffman et al. [47]
IMERG-Late	12 h	0.10° × 0.10°	Half-hourly	January 1998-present	Huffman et al. [47]
PDIR-Now	1 h	0.04° × 0.04°	Hourly	March 2000-present	Nguyen et al. [48]
PERSIANN-CCS	1 h	0.04° × 0.04°	Hourly	January 2003-present	Hong et al. [49]

The GPM mission developed an algorithm that combines microwave data from the GPM Microwave Imager (GMI) with observations from the Dual-frequency Precipitation Radar (DPR) and measurements from partner satellites. IMERG is generated from multiple satellite platforms and is available in three daily products: IMERG-Early, IMERG-Late, and IMERG-Final, with approximate latencies of 4 h, 12 h, and 3.5 months, respectively. In this study, we used the IMERG-Early and IMERG-Late products because they are classified as near-real-time products. The main difference between these products is latency and estimation methodology: IMERG-Early uses information from the most recently available satellites, whereas IMERG-Late incorporates data from satellites that were not available when the early version (IMERG-Early) was generated [47]. The IMERG data were downloaded from https://disc.gsfc.nasa.gov/, accessed on 20 September 2025.

The PDIR-Now algorithm estimates precipitation primarily from infrared (IR) data acquired by geostationary (GEO) satellites. Because it relies on IR observations, rainfall estimation is based on the indirect relationship between cloud-top temperature and precipitation rate. One of its main features is its ability to reduce bias through the dynamic shifting curve technique, which adjusts the position of the temperature–rainfall conversion curve using monthly climatological rainfall data [48]. This product has a spatial resolution of 0.04° × 0.04°. PERSIANN-CCS has the same spatial resolution and provides precipitation estimates every 30 min. This algorithm is also based on IR data and employs a cloud-patch classification system developed using computer vision and pattern recognition techniques [49]. PERSIANN data are available from https://chrsdata.eng.uci.edu/, accessed on 20 September 2025.

2.2.2. Observed Precipitation, Temperature, and Streamflow Data

Daily precipitation and temperature (minimum and maximum) records for the 1968–2014 period were obtained from 35 meteorological stations located within and along the basin's boundary (Figure 1, Table 2). Observed precipitation was used as input to the CEQUEAU model and as a reference dataset for evaluating the SPPs. In contrast, the observed temperature records were used only as model input. The meteorological stations are operated by the Comisión Nacional del Agua (CONAGUA: https://smn.conagua.gob.mx, accessed on 12 October 2025).

Table 2. Geographic characteristics and observation periods of the meteorological stations used in the TRB.

ID	Name	Long (° W)	Lat (° N)	Elevation (m a.s.l)	Data Period
7001	Abasolo Chiapas (CFE)	−92.217	16.833	1280	1970–2012
7006	Altamirano (SMN)	−92.058	16.741	1240	1968–2014
7022	Playas De Catazaja	−92.016	17.728	10	1968–2014
7028	Chacamax	−91.708	17.473	60	1969–2014
7042	El Carmen (CFE)	−91.617	16.767	929	1969–1994
7051	El Rosario (CFE)	−91.783	16.850	740	1968–1993
7064	Finca Morelia	−92.550	17.383	653	1968–1977
7071	Guaquitepec	−92.290	17.145	1160	1968–2014
7085	Palenque (SMN)	−91.982	17.509	60	1968–2014
7105	Las Nubes	−92.336	17.510	93	1968–2014
7107	Las Tazas (CFE)	−91.615	16.759	600	1968–1993
7108	Livingston (CFE)	−92.050	16.767	1200	1968–1994
7114	Yaquintela	−91.730	16.909	650	1968–2014
7122	Ocosingo	−92.066	16.933	865	1968–2014
7126	Palenque (DGE)	−91.983	17.567	60	1968–2014
7140	Sabana	−92.217	17.400	45	1968–1981
7141	Salto De Agua (DGE)	−92.334	17.575	10	1968–2014
7169	Tumbala (CFE)	−92.300	17.267	1063	1968–2014
7177	Yajalon (CFE)	−92.317	17.167	660	1968–2014
7179	Altamirano (CFE)	−92.000	16.683	1250	1968–1994
7192	Ocosingo (CFE)	−92.100	16.900	978	1968–1989
7195	Sabanilla (CFE)	−92.553	17.286	300	1972–2014
7196	Salto De Agua (SMN)	−92.333	17.550	124	1968–1969
7209	Agua Verde	−91.867	17.033	1240	1968–1969
7210	Finca Agua Azul (CFE)	−92.133	17.267	260	1968
7215	Altamirano (DGE)	−92.033	16.733	1240	1973–1990
7216	Bajada Grande	−92.261	17.701	20	1973–1990
7220	E.T.A. 259 Salto De Agua	−92.367	17.600	20	1973–1982
7315	Paso Del Cayuco (CFE)	−92.106	17.225	291	1977–2014
7324	Chacte (CFE)	−92.333	16.933	825	1978–1986
7356	Bachajon	−92.189	17.036	918	1982–1988
7389	Sitala	−92.307	17.022	1100	1984–2014
27004	Boca Del Cerro	−91.493	17.449	14	1968–2014
27046	Tenosique (DGE)	−91.421	17.503	19	1984–1985
27047	Tenosique (SMN)	−91.427	17.473	22	1968–2014

Daily mean streamflow records for the 1968–2014 period were obtained from the Salto de Agua hydrometric station. Hydrometric data were downloaded from the Sistema de Información Hidrológica (SIH) (https://sih.conagua.gob.mx/, accessed on 12 October 2025). These data were used to calibrate and validate the CEQUEAU model, which employs streamflow observations to adjust model parameters and verify the accuracy of the simulations, including those based on SPP estimates. Table 3 presents the location of the Salto de Agua hydrometric station.

Table 3. Geographic characteristics of the Salto de Agua hydrometric station.

Station	Geographic Coordinates		Basin Area (km^2)	Data Period
	Longitude	Latitude		
Salto de Agua	−92.333	17.559	3561	1968–2014

2.2.3. Land Use and Topography

Land-use information was produced by the Instituto Nacional de Estadística y Geografía (INEGI) and is available on the portal of the Comisión Nacional para el Conocimiento y Uso de la Biodiversidad (CONABIO). For this study, we used the 1:250,000-scale land-use

and vegetation map. This dataset is classified into several land use categories; however, it was necessary to reclassify the information into four categories: (i) lakes and water bodies, (ii) forests and tropical forests, (iii) marshes and wetlands, and (iv) others, because the CEQUEAU model requires this specific classification.

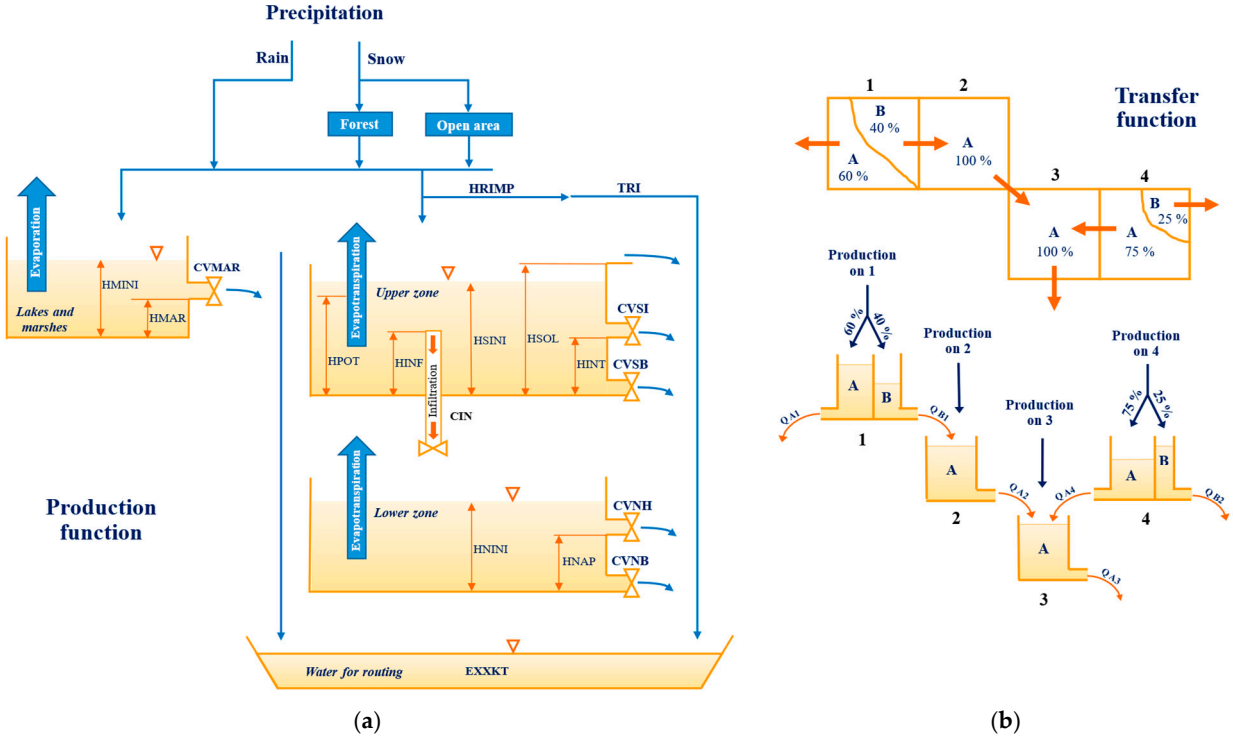
The Digital Elevation Model (DEM) of the study area was obtained from the Shuttle Radar Topography Mission (SRTM) product [50] with a spatial resolution of 30 × 30 m. This resolution provides higher terrain detail, enabling more precise processing tasks. The data are available from the SRTM Data Portal (https://srtm.csi.cgiar.org/srtmdata/, accessed on 30 November 2025).

2.3. CEQUEAU Hydrological Model

CEQUEAU is a distributed-parameter hydrological model that divides the watershed into elementary grid cells [51]. It was developed by the Institut National de la Recherche Scientifique–Eau, Terre et Environnement (formerly INRS-EAU, now INRS-ETE) at the University of Quebec, Canada. Discretizing the watershed into grid cells enables the model to calculate streamflow for each cell while accounting for the spatiotemporal variability of the watershed's physiographic characteristics [52,53]. The CEQUEAU model can estimate streamflow at both gauged and ungauged locations within the watershed and can simulate artificial storage systems.

CEQUEAU is structured around two main modules that together represent the runoff generation process from the moment water reaches the watershed surface to the outlet point (hydrometric station). The first module, called the production function (Figure 2a), is responsible for modeling the vertical water fluxes (precipitation, evapotranspiration, infiltration, etc.) and calculating the water volume stored in the three reservoirs considered by CEQUEAU: (i) lakes and wetlands, (ii) soil, and (iii) aquifers.

The transfer function (Figure 2b), in turn, analyzes flow routing through the drainage network and considers the influence of lakes, wetlands, and artificial infrastructure such as dams and diversions, among others [54].



(**a**) (**b**)

Figure 2. Modules of the CEQUEAU model: (**a**) production function; (**b**) transfer function [55].

To perform the simulations, the CEQUEAU model requires, in addition to the hydrometeorological database, four input files: (i) the model parameter file (.PAH), (ii) the hydrometeorological data file (.DHM), (iii) the physiographic data file (.PHY), and (iv) the watershed data file (.BV) [54]. These files can be generated either manually or automatically using the CEQUEAU-TerrSet module available in the TerrSet 2020 software. This module requires: (i) a DEM, (ii) the watershed boundary, (iii) the location of the hydrometric station, (iv) the location of the meteorological stations, and (v) a reclassified land use image in the format required by CEQUEAU. The CEQUEAU-TerrSet hydrogeomatic module generates a project file for execution in CEQUEAU, specifying the paths to all files required for processing [53].

3. Methodology

Because precipitation is one of the most important input variables in hydrological models, this study incorporated three precipitation datasets: observed precipitation from 35 meteorological stations, original SPP estimates, and SPP estimates corrected using the LS method. For this purpose, precipitation values from the SPP pixels at each meteorological station's location were extracted, enabling both evaluation and bias correction of the SPPs.

3.1. Evaluation of Satellite Precipitation Product Estimates

3.1.1. Basin-Scale Scatter Plots

Scatter plots were used to assess the linear relationship between SPP estimates and observed precipitation data. This analysis was performed at the monthly and areal scales, where each point represents a pair of values (observed precipitation on the X-axis and SPP estimate on the Y-axis). In addition, the 1:1 line was used to identify whether the SPP tends to overestimate or underestimate the observed records.

3.1.2. Descriptive Statistics

Descriptive statistics indicate differences between SPP estimates and observed records. Common descriptive statistics used to evaluate SPPs include the Pearson correlation coefficient (PCC), mean absolute error (MAE), Nash–Sutcliffe efficiency (NSE), and percent bias (PB) [56–59]. The equations and value ranges of these statistics are summarized in Table 4.

Table 4. Equations and evaluation criteria for the statistical metrics used to assess SPP performance.

Equation	Range	Best Value
$PCC = \frac{\sum(G-\overline{G})(S-\overline{S})}{\sqrt{(G-\overline{G})^2}\sqrt{(S-\overline{S})^2}}$	−1 a 1	−1 or 1
$MAE = \frac{1}{N}\sum(\lvert S-G\rvert)$	0 a ∞	0
$NSE = 1-\frac{\sum(S-G)^2}{\sum(G-\overline{G})^2}$	−∞ a 1	1
$PB = 100\times\frac{\sum(G-S)}{\sum G}$	−∞ a ∞	0

G: meteorological station observations (mm); $\overline{G}$: mean meteorological station observations (mm); S: SPP estimates for the analyzed pixel (mm); $\overline{S}$: mean SPP estimate (mm); and N: number of data pairs.

3.2. Bias Correction of SPPs

Bias correction was performed using the LS method, which reduces systematic differences between SPP estimates and observed precipitation. These differences can affect the accuracy of hydrological analyses; therefore, SPPs must be corrected before being applied in hydrological models [36,60]. The LS method calculates a monthly scaling factor to apply to the SPP daily precipitation estimates. In other words, each daily estimate was multiplied by

the scaling factor for its month, ensuring that the mean of the corrected values is consistent with the observed data (Equation (1)).

$$P_{SCorr(d)} = P_{S(d)} \frac{\overline{P_{G(m)}}}{\overline{P_{S(m)}}} \quad (1)$$

$P_{SCorr(d)}$: is the bias-corrected daily precipitation of the SPP; $P_{S(d)}$: is the uncorrected daily precipitation of the SPP; $\overline{P_{G(m)}}$: is the observed mean monthly precipitation (meteorological stations); and $\overline{P_{S(m)}}$: is the mean monthly precipitation of the SPP.

The bias correction was performed based on the relationship between the SPP pixel containing each meteorological station and the corresponding observed precipitation record. In this way, the satellite estimates were adjusted based on the corresponding observed records, enabling a more accurate correction by better representing local conditions. The observed and SPP mean monthly precipitation were calculated using a subroutine incorporated into the CEQUEAU hydrological model [61].

3.3. Streamflow Simulation Using the CEQUEAU Model

Table 5 summarizes the geospatial and hydrometeorological datasets used in the CEQUEAU version 4.0 modeling process. The CEQUEAU-TerrSet hydrogeomatic module processes these datasets to generate the CEQUEAU project files required to run the model [53].

Table 5. Summary of datasets used for hydrological modeling with CEQUEAU.

Dataset	Format	Spatial/Temporal Resolution	Analysis Period	Purpose
Geospatial datasets				
Digital Elevation Model (DEM)	Raster	30 m	—	Hydrogeomatic preprocessing
Land use	Raster	30 m	—	Hydrogeomatic preprocessing
Watershed boundary	Vector	—	—	Hydrogeomatic preprocessing
Meteorological station locations	Vector	—	—	Hydrogeomatic preprocessing
Hydrometric station location	Vector	—	—	Hydrogeomatic preprocessing
Hydrometeorological datasets				
Observed precipitation	ASCII	Daily	1968–2014	Streamflow simulation
SPPs	ASCII	Daily	2003–2014	Streamflow simulation
Maximum and minimum temperature	ASCII	Daily	1968–2014	Streamflow simulation

Three types of precipitation data were used to simulate streamflows with CEQUEAU: (i) observed records from meteorological stations, (ii) original SPP estimates, and (iii) bias-corrected SPP estimates. CEQUEAU uses precipitation values assigned to input points rather than working directly with pixels; consequently, the SPP estimates were associated with the same 35 meteorological station locations used for observed precipitation. The basin was discretized into 4 × 4 km grid cells for the CEQUEAU model. For each SPP, the precipitation value was extracted from the pixel containing each meteorological station's location, preserving the original spatial resolution of each product: 0.04° × 0.04° for PERSIANN-CCS and PDIR-Now, and 0.10° × 0.10° for IMERG-Early and IMERG-Late. Thus, the SPPs were not resampled to a common spatial resolution; instead, their precipitation estimates were used as inputs in CEQUEAU at the same reference points.

In the first stage, meteorological station data were used for model calibration (1991–2014) and validation (1968–1990). In contrast, the calibration and validation periods for the SPPs datasets were 2003–2011 and 2012–2014, respectively. This was because SPP estimates exhibit temporal differences relative to observed data, potentially altering

the simulated hydrological response. Therefore, it is important to recalibrate the CEQUEAU parameters to ensure an adequate representation of hydrological behavior under the conditions associated with each precipitation source.

3.3.1. Calibration and Validation of the CEQUEAU Model

CEQUEAU employs several parameters (Figure 2a) associated with different phases of the hydrological cycle (precipitation, infiltration, runoff, evaporation, etc.) that must be calibrated to simulate streamflows. However, depending on the region, some parameters may not be considered. For example, in the TRB, snow-related parameters were not calibrated. Table 6 presents the parameter values obtained from calibrating the CEQUEAU model for the Tulijá River Basin (TRB), using precipitation data from meteorological stations for the 1991–2014 period. We calibrated 19 parameters and subsequently used the resulting values to validate the model for the 1968–1990 period. These values were also used as initial values for calibrating the model with each satellite precipitation product (SPP). Section 4 presents the hydrographs and performance metrics for the calibration and validation periods of each SPP.

Table 6. Calibrated parameter values of the CEQUEAU model using meteorological station data.

N	Parameter Name	Description	Value
1	CIN	Infiltration coefficient in the LOWER ZONE reservoir	0.12
2	CVNB	Low draining coefficient of the LOWER ZONE reservoir	0.01
3	CVNH	High draining coefficient of the LOWER ZONE reservoir	0.03
4	CVSB	Low draining coefficient of the UPPER ZONE reservoir	0.019
5	CVSI	Intermediate draining coefficient of the UPPER ZONE reservoir	0.216
6	HINF	Infiltration threshold of the UPPER ZONE reservoir towards the LOWER ZONE reservoir (mm)	26.510
7	HINT	Intermediate draining threshold of the UPPER ZONE reservoir (mm)	50
8	HNAP	Threshold of high draining of the LOWER ZONE reservoir (mm)	165.50
9	HRIMP	Depth of water required to begin the runoff on impervious surfaces (mm)	1
10	HSOL	Height of the UPPER ZONE reservoir (mm)	213.504
11	EVNAP	Fraction of the evaporation-transpiration taken in the LOWER ZONE reservoir (from 0.0 to 1.0)	0.3
12	HPOT	Threshold of water taken away at a potential rate by evapotranspiration (mm)	86.333
13	XAA	Exponent of Thornthwaite formula	2.73
14	XIT	Value of Thornthwaite thermal index	121.14
15	EXXKT	Adjustment parameter of the transfer coefficients from a partial square to the next, for a time step of one day	0.001
16	COET	Correction of the temperatures according to altitude (°C/1000 m)	0.0
17	COEP	Correction of the precipitation according to altitude (mm/meter/year)	0.0
18	XINFMA	Maximum infiltration (mm/time step)	20
19	TRI	Fraction of impervious area on whole squares (from 0.0 to 1.0)	0.008

CEQUEAU was calibrated using two techniques: a trial-and-error procedure and automatic optimization with the Best Overall Transferable Model (BOTM). In the first technique, parameter values were manually adjusted until the observed and simulated annual

runoff depths became as similar as possible. Once these parameter ranges were identified, automatic calibration was performed using the BOTM tool, which is the calibration method implemented in CEQUEAU. BOTM is based on the Powell algorithm, a deterministic method that does not require derivative calculations and allows the simultaneous optimization of multiple parameters. This approach improves calibration efficiency by reducing computational time and minimizing bias from manual adjustments. Subsequently, the model was validated by verifying the parameters obtained during calibration; that is, the model was run again using a different data period [61].

3.3.2. Performance Evaluation of the CEQUEAU Model

Hydrological simulations for all scenarios were evaluated using three statistical criteria: the Nash–Sutcliffe Efficiency coefficient (NSE), Percent Bias (PBIAS), and the coefficient of determination (R^2). Table 7 presents the statistical metrics and the criteria used to interpret them. NSE is a normalized indicator that determines the relative magnitude of the residual variance compared to the variance of the observed data. PBIAS measures the model's systematic tendency to overestimate or underestimate observed streamflows. The smaller the magnitude of PBIAS, the more reliable the simulation. R^2 evaluates the degree of agreement between simulated and observed streamflows, reflecting the proportion of variability in observed streamflows that the model can explain. However, this statistic can be highly sensitive to extreme values and insensitive to additive or proportional differences between simulated and observed data [62].

Table 7. Evaluation criteria for the statistical metrics used to assess CEQUEAU model performance.

Statistical Metric	Performance Classification According to Moriasi et al. [62]			
	Very Good	**Good**	**Satisfactory**	**Not Satisfactory**
NSE	NSE > 0.80	0.70 < NSE ≤ 0.80	0.50 < NSE ≤ 0.70	NSE ≤ 0.50
PBIAS	PBIAS < ±5	±5 ≤ PBIAS < ±10	±10 ≤ PBIAS < ±15	PBIAS ≥ ±15
R^2	R^2 > 0.85	0.75 < R^2 ≤ 0.85	0.60 < R^2 ≤ 0.75	R^2 ≤ 0.60

4. Results

This section presents the study's results in two main parts. First, the precipitation estimates from the four near-real-time SPPs (IMERG-Early, IMERG-Late, PERSIANN-CCS, and PDIR-Now) are evaluated against observed precipitation at monthly and areal scales using graphical analysis and descriptive statistics, followed by the application of bias correction using the LS method. Second, the daily streamflow simulation results are presented for three precipitation datasets: observed precipitation, original SPP estimates, and bias-corrected SPP estimates, all processed using the CEQUEAU hydrological model.

4.1. Graphical Evaluation of SPPs Versus Observed Precipitation

The evaluation of the four SPPs used observed records from meteorological stations at the monthly and areal scales for the period beginning in 2003, when PERSIANN-CCS data became available. At the areal scale, the observed and estimated mean monthly precipitation in the TRB were calculated using a subroutine integrated into the CEQUEAU model, based on Thiessen polygons.

Figure 3 shows scatter plots of observed precipitation versus SPP estimates. IMERG-Late exhibited the highest R^2 value (0.59), with a distribution closer to the 1:1 line, followed by PDIR-Now (R^2 = 0.56) and IMERG-Early (R^2 = 0.55), whose estimates showed greater dispersion during intense rainfall events. In contrast, PERSIANN-CCS showed the lowest R^2 value (0.51) and considerable dispersion across the precipitation range. Overall, IMERG-Early and IMERG-Late tended to underestimate precipitation, whereas PDIR-Now tended to overestimate it. PERSIANN-CCS showed greater variability in its estimates.

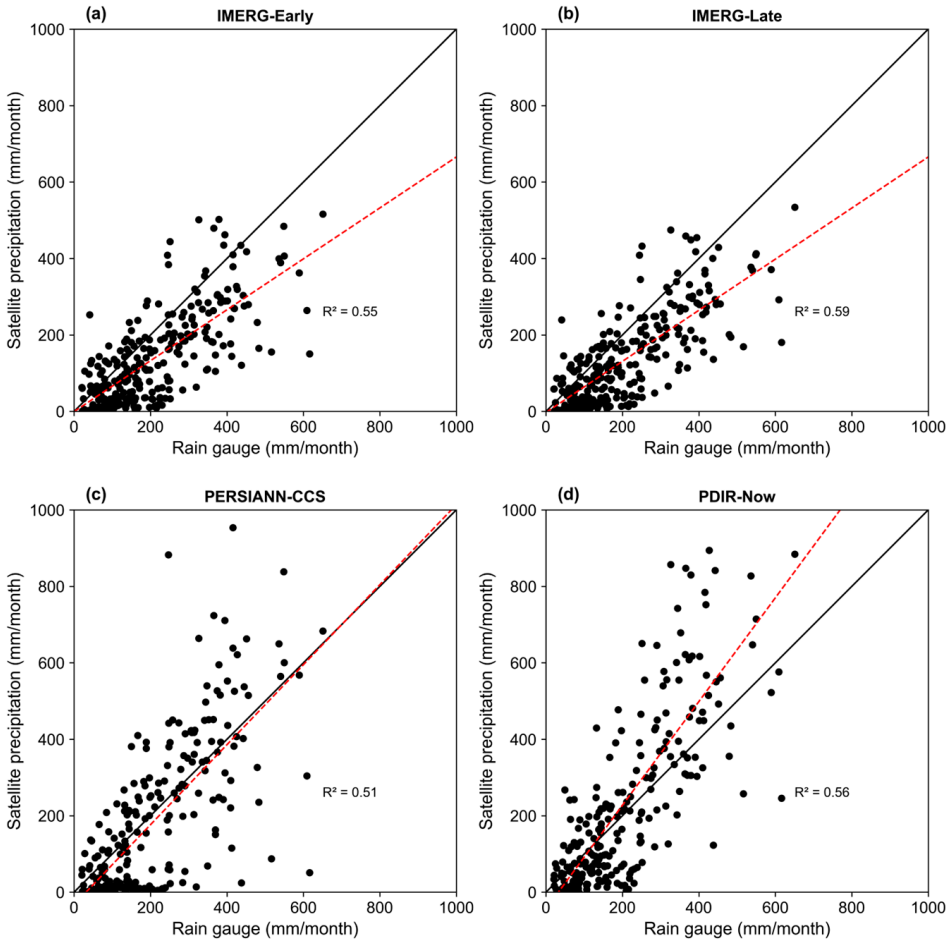


Figure 3. Scatter plots of the observed and estimated mean monthly precipitation for each SPP at the basin scale: (**a**) IMERG-Early, (**b**) IMERG-Late, (**c**) PERSIANN-CCS, and (**d**) PDIR-Now. The black solid line represents a 1:1 relation, and the red dashed line represents the fitted linear regression.

These differences may be associated with the latency of the SPPs, since they are generated in near-real-time. Therefore, their processing is limited, as they do not include subsequent adjustments applied to other SPPs. In this sense, although the SPPs adequately captured monthly variability, their direct application in hydrological modeling could introduce errors in streamflow simulations.

Figure 4 presents the areal mean monthly precipitation. It can be observed that all SPPs adequately reproduced the rainfall seasonality in the TRB throughout the different months of the year. However, systematic biases in precipitation magnitude were identified. During the dry months, the SPPs tended to underestimate rainfall, showing better performance in April and May. In contrast, during the wettest months, bias magnitude and direction varied among the SPPs, with pronounced overestimation in some products, particularly in June and September.

IMERG-Early and IMERG-Late showed the best performance in capturing rainfall over several months (March to August), with estimates closer to rain-gauge records, though slightly underestimating rainfall during the wettest months (September and October). PERSIANN-CCS estimates showed good agreement only in April and May. In contrast, PDIR-Now underestimated precipitation during the dry season and considerably overestimated rainfall during the rainy season. Therefore, the IMERG-Early and IMERG-Late products showed greater month-to-month stability.

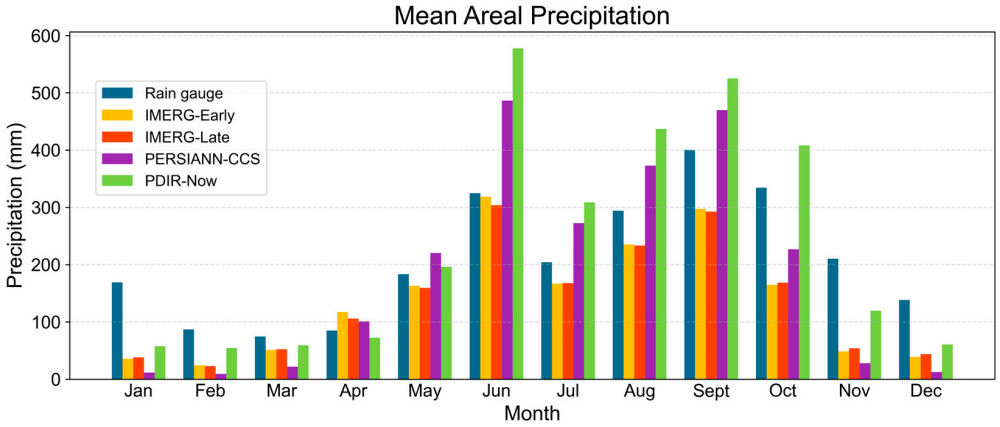


Figure 4. Comparison between the observed and SPP-estimated mean monthly precipitation in the TRB.

4.2. Evaluation of SPP Performance Using Descriptive Statistics

Figure 5 presents the monthly descriptive statistics. For the PCC, all SPPs except PERSIANN-CCS showed good performance, with correlations ranging from 0.47 to 0.83. Both IMERG products performed best, with median values around 0.70, though IMERG-Late was slightly superior. In contrast, PERSIANN-CCS showed greater dispersion, including lower values compared to the other SPPs. For the MAE, where lower values indicate better SPP performance, both IMERG-Early and IMERG-Late achieved the best results, with relatively low MAE values, indicating smaller errors between their estimates and precipitation recorded by meteorological stations. In contrast, PDIR-Now performed the poorest, with a median around 140 mm and values up to 180 mm, indicating substantial estimation errors.

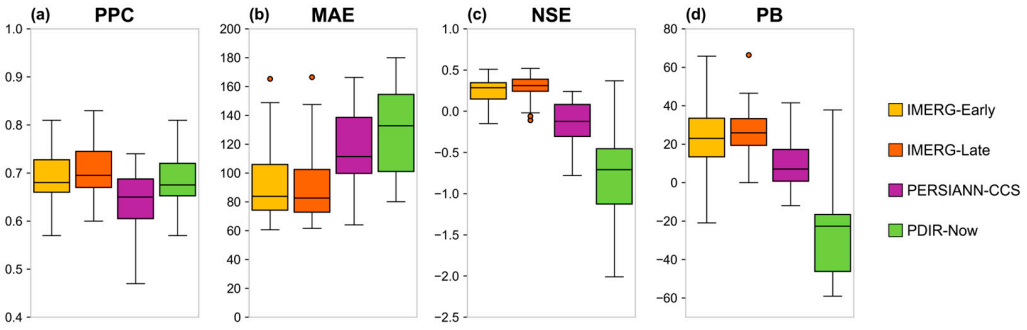


Figure 5. Monthly performance metrics for each SPP: (**a**) Pearson correlation coefficient, (**b**) mean absolute error, (**c**) Nash–Sutcliffe efficiency, and (**d**) percent bias.

For NSE, the IMERG products performed well, with NSE values near 0.50 and consistent performance across both SPPs. However, PERSIANN-CCS and PDIR-Now exhibited negative NSE values, with PDIR-Now showing the lowest values. Regarding Percent Bias (PB), where values close to zero indicate the absence of systematic bias, PDIR-Now showed a clear tendency to overestimate, with PB values reaching 60%. In contrast, IMERG-Early, IMERG-Late, and PERSIANN-CCS showed underestimation. Nevertheless, IMERG-Late presented PB values closer to zero, indicating better agreement with the observed precipitation.

Overall, IMERG-Late performed best among all SPPs. Conversely, PDIR-Now performed the poorest, with extremely negative NSE values and pronounced overestimation in Percent Bias (PB). Although it showed an acceptable correlation (PCC), its high bias and large errors led to poor overall performance.

4.3. Bias Correction

Bias correction was performed using the LS method at the daily scale in the TRB for all SPPs. Table 8 presents the monthly correction coefficients for each SPP, calculated as the ratio of the observed interannual monthly precipitation to the precipitation estimated by each product. During April to September, the coefficients ranged from 0.72 to 1.42, indicating that the different SPPs estimated monthly precipitation with acceptable accuracy during the wet season. However, from October to March, the coefficients ranged from 0.98 to 92.45, reflecting substantial differences between observed precipitation and SPP estimates, particularly for PERSIANN-CCS, which presented the highest correction factors. This occurs because during months with little or no precipitation, SPPs tend to underestimate rainfall amounts, leading to much larger correction coefficients when compensating for low precipitation estimates under dry conditions.

Table 8. Monthly LS bias-correction coefficients for the SPP estimates.

SPP	Jan	Feb	Mar	Apr	May	Jun	Jul	Aug	Sept	Oct	Nov	Dec
IMERG-Early	10.31	11.99	4.72	0.77	1.18	1.08	1.35	1.35	1.41	2.24	7.33	8.39
IMERG-Late	9.30	8.65	3.96	0.84	1.22	1.13	1.32	1.37	1.42	2.16	6.59	8.46
PERSIANN-CCS	44.95	92.45	12.37	0.97	0.90	0.72	0.80	0.83	0.92	1.90	30.82	31.87
PDIR-Now	7.88	13.89	24.19	1.42	1.08	0.63	0.80	0.77	0.86	0.98	3.21	6.47

Table 9 presents the statistical properties of the average monthly areal precipitation for the TRB, based on observed data and both original and bias-corrected SPPs. Following bias correction, the mean monthly precipitation for all SPPs approached the observed value (210.6 mm month^{-1}), reflecting the Linear Scaling method's objective of reducing systematic bias by adjusting mean precipitation.

Table 9. Statistical properties of observed, original SPP, and LS-corrected SPP monthly areal precipitation in the TRB during 2003–2014.

Dataset	Mean (mm Month^{-1})	Std. Dev. (mm Month^{-1})	Max (mm Month^{-1})
Observed precipitation	210.6	141.6	650.8
IMERG-Early	147.2	133.6	516.2
IMERG-Early bias-corrected	216.5	144.1	662
IMERG-Late	144.6	129.2	534.1
IMERG-Late bias-corrected	217.3	143.4	661.5
PERSIANN-CCS	184.1	205.9	882.7
PERSIANN-CCS bias-corrected	199.3	148.9	648.8
PDIR-Now	259.9	274.6	1343.3
PDIR-Now bias-corrected	206.9	143.4	648.9

Cumulative distribution function (CDF) plots were generated at the monthly and areal scales, both before and after bias correction, to visualize the data adjustment. Figure 6 shows that both IMERG products exhibited similar behavior: the distributions of the SPPs before correction indicated underestimation in the low and medium precipitation ranges, whereas for high precipitation values they tended to approach the observed precipitation distribution. However, after applying the LS correction, the distributions of the corrected SPPs showed a notable agreement with the observed precipitation distribution, demonstrating better performance within the 0–450 mm/month range.

For the PERSIANN products, although they generally exhibited similar behavior, important differences were observed. For PERSIANN-CCS, a more pronounced overestimation was identified in the medium and high precipitation ranges, reaching values close to

1000 mm/month, which were not present in the observed records. After applying the LS correction, the corrected CDF became more consistent with the CDF of the observed precipitation, although differences remained for lower precipitation values within the 0–250 mm/month range. In contrast, PDIR-Now slightly underestimated low-precipitation events; however, it showed the largest overestimation for accumulations exceeding 1200 mm/month, indicating a substantial bias relative to the observed precipitation.

After bias correction, the corrected data distribution improved considerably and became more consistent with the observed distribution. Therefore, the correction substantially reduced the bias, reinforcing its usefulness for hydrological modeling applications in the study area.

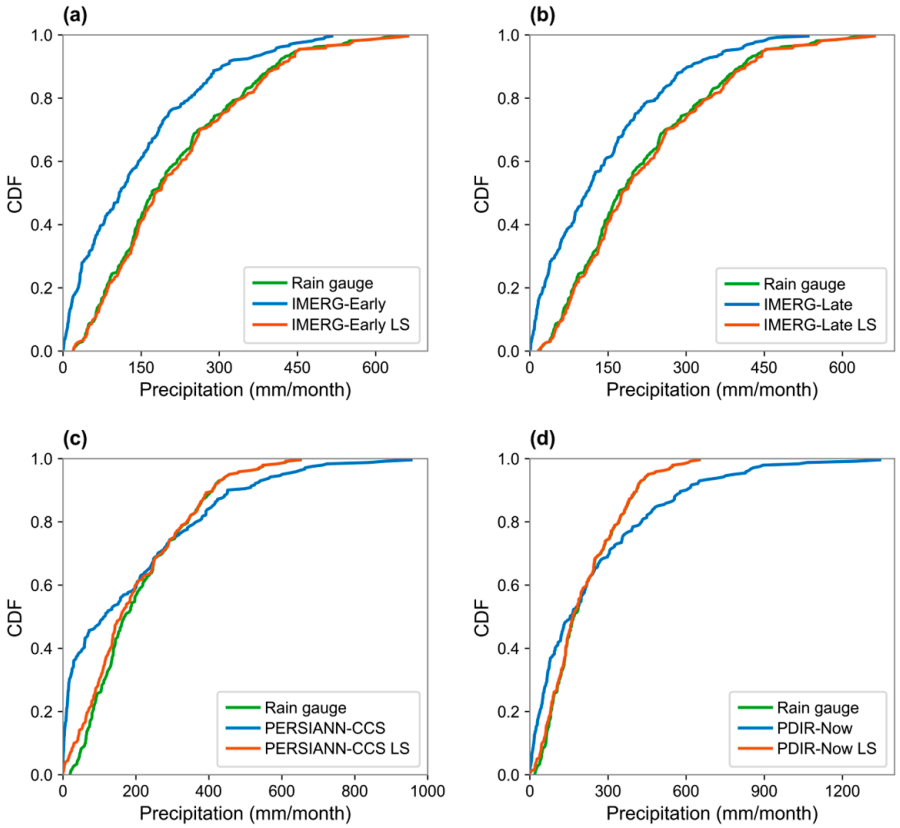


Figure 6. Cumulative distribution functions (CDFs) of observed precipitation and original and LS-corrected SPP estimates at the monthly scale: (**a**) IMERG-Early, (**b**) IMERG-Late, (**c**) PERSIANN-CCS, and (**d**) PDIR-Now.

4.4. Daily Streamflow Simulation Using the CEQUEAU Model

4.4.1. Hydrological Modeling with CEQUEAU Using Observed Precipitation

The CEQUEAU model was calibrated using observed precipitation data for the 1991–2014 period and validated for the 1968–1990 period. Table 10 presents the statistical criteria values for each year. At the daily scale, the model showed good to very good performance across most years, with NSE values exceeding 0.5. In addition, NSE values did not decrease over time, indicating that CEQUEAU maintained stable simulation capability throughout the study period. The lowest annual NSE values were recorded in 1991 (0.36) and 2012 (0.37), mainly because the model struggled to reproduce the largest streamflow peaks. Because NSE is sensitive to errors in high flows, underestimating these events reduced the model's annual performance.

Regarding PBIAS, results ranged from 36% to −9%, with a general tendency toward underestimating observed streamflows. Nevertheless, most values remained within the

acceptable range (±15%), according to the criteria proposed by Moriasi et al. [62]. During the calibration period (1991–2014), the model performed consistently, whereas during the validation period (1968–1990), greater interannual variability was observed, although an adequate fit was still maintained. Overall, the results indicate that CEQUEAU consistently reproduces the TRB hydrological response when using observed precipitation data, despite the limited distribution of meteorological stations, particularly in the rainiest area of the TRB.

Figure 7 presents hydrographs of observed and simulated daily streamflows using observed precipitation for the calibration and validation periods, along with the overall performance metrics for each period. CEQUEAU demonstrated near-good performance in both calibration and validation. During calibration, the model achieved an NSE of 0.66, an R^2 of 0.70, and a PBIAS of 17.15% (Figure 7a), whereas during validation, the model achieved an NSE of 0.69, an R^2 of 0.71, and a PBIAS of 12.54% (Figure 7b). In both periods, positive PBIAS values were obtained, indicating underestimation of streamflows, although the PBIAS performance was classified as good according to the criteria proposed by Moriasi et al. [62]. The hydrographs for both periods show good agreement between observed and simulated streamflows, adequately reproducing the temporal variability and peak flows during the wet season, although with slight underestimation in some maximum flow events.

Table 10. Annual performance metrics of daily streamflow simulations using observed precipitation.

Validation Period				Calibration Period			
Year	**NSE**	**R^2**	**PBIAS**	**Year**	**NSE**	**R^2**	**PBIAS**
1968	0.71	0.67	11.19	1991	0.36	0.31	21.10
1969	0.78	0.67	6.56	1992	0.76	0.80	1.96
1970	0.78	0.74	0.48	1993	0.54	0.46	−0.38
1971	0.70	0.76	6.76	1994	0.72	0.82	−9.59
1972	0.62	0.58	6.89	1995	0.79	0.72	1.17
1973	0.82	0.78	2.02	1996	0.51	0.54	−9.01
1974	0.73	0.77	6.73	1997	0.49	0.59	25.92
1975	0.72	0.66	1.82	1998	0.70	0.76	15.20
1976	0.63	0.63	15.49	1999	0.67	0.74	33.85
1977	0.69	0.70	5.30	2000	–	–	–
1978	0.73	0.67	7.41	2001	–	–	–
1979	0.59	0.58	3.42	2002	–	–	–
1980	0.75	0.71	−0.67	2003	0.58	0.71	15.26
1981	0.63	0.75	22.70	2004	0.60	0.61	17.16
1982	0.69	0.53	15.75	2005	0.69	0.69	14.89
1983	0.59	0.47	9.75	2006	0.64	0.54	16.38
1984	0.73	0.75	20.83	2007	0.59	0.75	27.78
1985	0.44	0.55	29.66	2008	0.72	0.75	21.09
1986	0.42	0.54	25.49	2009	0.41	0.54	31.81
1987	–	–	–	2010	0.48	0.40	36.00
1988	0.74	0.83	13.43	2011	0.78	0.81	25.97
1989	–	–	–	2012	0.37	0.32	13.60
1990	0.46	0.70	35.92	2013	0.68	0.62	17.55
				2014	0.62	0.68	17.32

Note. Dashes (–) indicate that the performance metrics were not calculated for those years due to the lack of available hydrometric records for the evaluation.

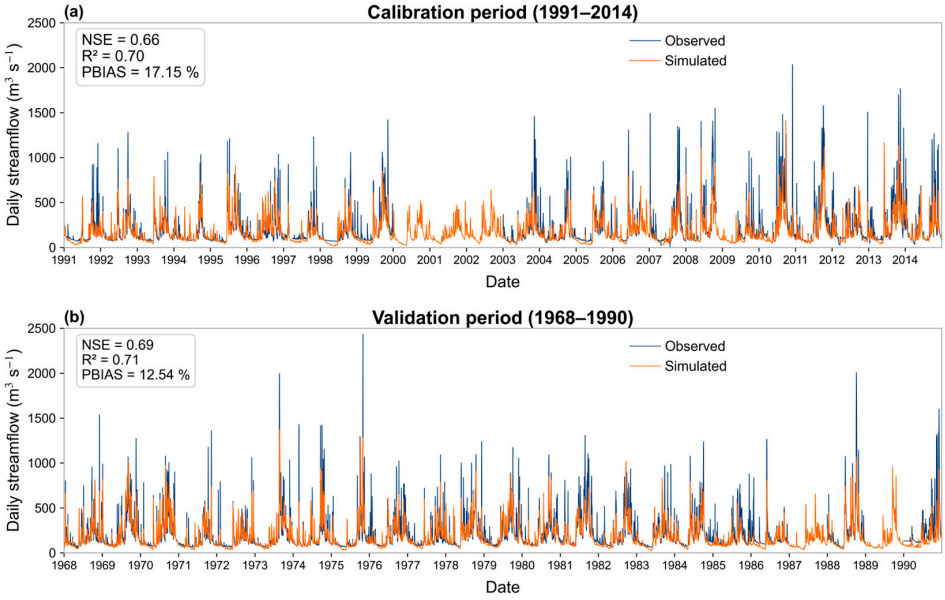


Figure 7. Hydrographs of observed and simulated daily streamflows using observed precipitation: (**a**) calibration (1991–2014) and (**b**) validation (1968–1990).

4.4.2. CEQUEAU Modeling Using Near-Real-Time SPPs

CEQUEAU was recalibrated to simulate streamflow in the TRB using estimates from four near-real-time SPPs. Calibration was performed for 2003–2011, while validation was conducted for 2012–2014. Table 11 summarizes the scores obtained for the three statistical criteria. Based on the NSE results, all SPPs showed poor performance in simulating daily streamflows in the TRB, with values below 0.5, which Moriasi et al. [62] classify as unsatisfactory. Negative NSE values were even observed, particularly for the PERSIANN-CCS y PDIR-Now.

Table 11. Annual performance metrics of daily streamflow simulations using original near-real-time SPP estimates.

Year	IMERG-Early			IMERG-Late			PERSIANN-CCS			PDIR-Now		
	NSE	R^2	PBIAS	NSE	R^2	PBIAS	NSE	R^2	PBIAS	NSE	R^2	PBIAS
2003	−0.08	0.11	41.43	−0.01	0.17	43.56	−2.33	0.02	−10.89	−10.21	0.07	−79.14
2004	−0.01	0.23	41.74	−0.06	0.23	46.24	−0.04	0.19	37.70	−0.14	0.28	1.61
2005	0.33	0.50	30.66	0.32	0.49	32.40	−0.90	0.40	−10.46	−6.67	0.33	−63.11
2006	0.24	0.25	7.98	0.18	0.20	12.79	−0.22	0.24	−25.58	−3.42	0.05	−87.56
2007	0.06	0.27	49.68	0.05	0.28	50.90	−0.27	0.15	21.74	−2.76	0.19	−17.64
2008	0.28	0.50	41.39	0.28	0.53	41.89	0.33	0.39	21.81	−0.13	0.35	−12.88
2009	0.11	0.19	14.82	0.18	0.23	12.31	0.34	0.37	22.75	0.35	0.37	−3.65
2010	0.36	0.53	39.90	0.37	0.59	42.71	−0.17	0.40	6.51	−3.56	0.31	−49.43
2011	0.12	0.25	36.97	0.25	0.36	37.40	−0.15	0.23	31.91	−2.25	0.14	−6.53
2012	−0.24	0.14	40.63	−0.19	0.17	43.90	−1.04	0.06	24.42	−4.25	0.06	−14.82
2013	0.02	0.32	52.02	0.06	0.35	50.43	−0.18	0.19	30.14	−0.55	0.27	−2.77
2014	−0.17	0.29	60.99	−0.14	0.33	60.48	0.01	0.23	41.06	0.06	0.29	18.98

R^2 values ranged from 0.02 to 0.59, indicating that the SPP-estimated streamflows were unable to adequately reproduce the temporal variability of the observed streamflows, compared with those simulated from observed precipitation. In addition, large PBIAS values were observed. The IMERG products with positive PBIAS values tended to underestimate observed streamflows, as did PERSIANN-CCS; in contrast, PDIR-Now tended to overestimate streamflows. Overall, the IMERG products performed the worst on this statistical criterion.

Figure 8 presents the hydrographs of observed and simulated daily streamflows using the estimates from each SPP for both the calibration and validation periods. CEQUEAU performed poorly in streamflow simulation when using SPP estimates, compared with results obtained with observed precipitation. In general, NSE and R^2 values were low during both calibration and validation, indicating that near-real-time SPP estimates have limited capacity to reproduce the TRB observed streamflow dynamics.

Throughout the calibration period, the model produced NSE values of 0.16–0.17 for IMERG-Early and IMERG-Late. In contrast, both products produced negative NSE values over the entire validation period, with positive PBIAS values (>33%) indicating a tendency to underestimate observed streamflows (Figure 8a,b). PERSIANN-CCS and PDIR-Now showed negative NSE values and low R^2 values during both calibration and validation (Figure 8c,d). Their overall PBIAS values were lower in magnitude than those obtained with the IMERG products. Visually, the hydrographs showed poor agreement between observed and simulated streamflows, especially during flood periods; the IMERG products tended to underestimate peak flows, whereas PDIR-Now showed a pronounced overestimation of several peak flow events. PERSIANN-CCS showed a more variable behavior. Overall, these results demonstrate that uncorrected SPP estimates are insufficient to reproduce the TRB hydrological response. This behavior may be associated with systematic errors, the limited latency of near-real-time products, and the region's complex topography.

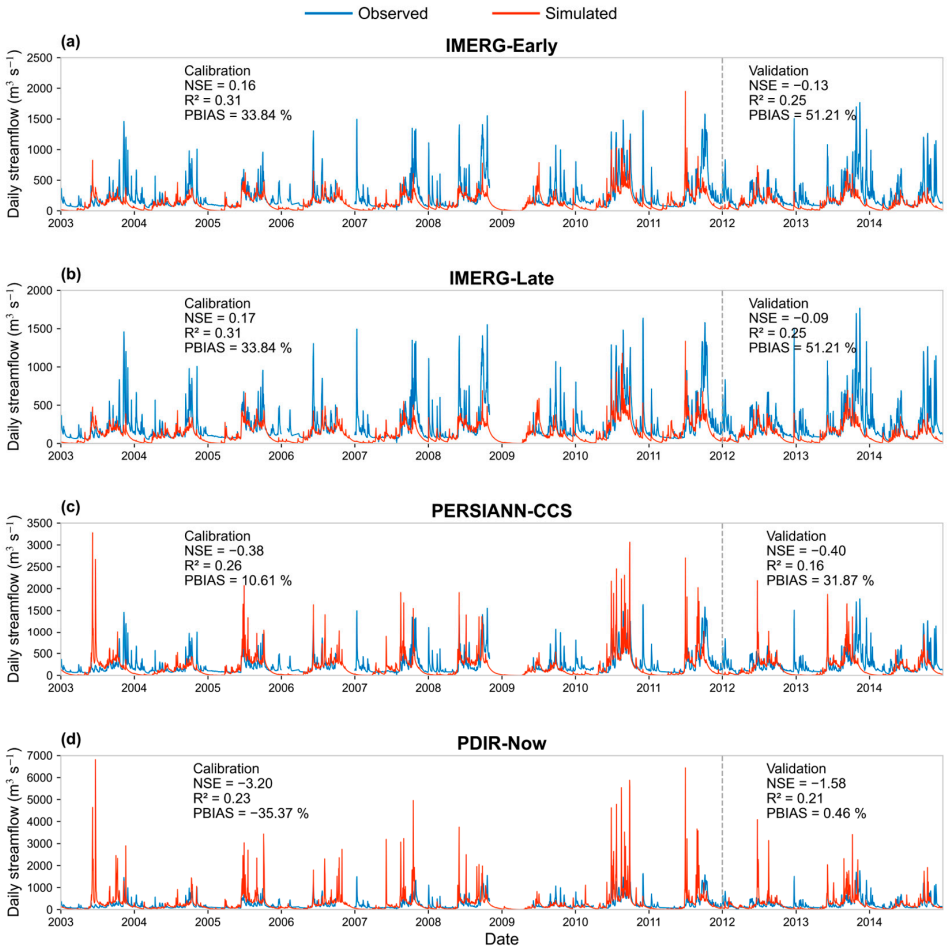


Figure 8. Hydrographs of observed and simulated daily streamflows using original SPP estimates during the calibration (2003–2011) and validation (2012–2014) periods: (**a**) IMERG-Early, (**b**) IMERG-Late, (**c**) PERSIANN-CCS, and (**d**) PDIR-Now. The vertical dashed line indicates the transition between the calibration (2003–2011) and validation (2012–2014) periods.

4.4.3. CEQUEAU Modeling Using Bias-Corrected Near-Real-Time SPPs

The performance of CEQUEAU for simulating daily streamflows in the TRB was evaluated using estimates from the four SPPs after bias correction. Table 12 summarizes the statistical criteria obtained for each product. Overall, the NSE and R^2 values indicate that the streamflows simulated with the corrected IMERG-Early and IMERG-Late products performed better than those simulated with the corrected PERSIANN-CCS and PDIR-Now. The IMERG products achieved NSE values of 0.40–0.74 and R^2 values of 0.41–0.79, indicating CEQUEAU's good ability to reproduce the temporal variability of observed streamflows. In contrast, the PERSIANN-CCS and PDIR-Now products showed lower interannual consistency, with NSE values below 0.5 for most years, suggesting limitations in representing the magnitude and distribution of precipitation even after bias correction.

According to the PBIAS statistic, which assesses the model's tendency to overestimate or underestimate streamflow, IMERG-Early and IMERG-Late performed from satisfactory to very good according to the criteria proposed by Moriasi et al. [62]. In most years, the four SPPs tended to underestimate observed streamflows. These results indicate that, despite the improvement achieved through bias correction, the SPPs still retained systematic biases in precipitation estimation, which directly affected the simulated streamflows. Overall, the results indicate that IMERG-Late and IMERG-Early are the most suitable products for daily hydrological simulation with CEQUEAU in the TRB, as they exhibit greater interannual stability and lower bias.

Table 12. Annual performance metrics of daily streamflow simulations using LS-corrected SPP estimates.

Year	IMERG-Early LS			IMERG-Late LS			PERSIANN-CCS LS			PDIR-Now LS		
	NSE	R^2	PBIAS	NSE	R^2	PBIAS	NSE	R^2	PBIAS	NSE	R^2	PBIAS
2003	0.51	0.53	−5.58	0.58	0.58	−4.96	0.43	0.45	4.39	0.46	0.46	−0.31
2004	0.46	0.50	−16.84	0.45	0.49	−15.28	0.45	0.47	−6.09	0.42	0.43	−10.11
2005	0.50	0.63	−10.56	0.51	0.63	−7.56	0.37	0.57	−7.58	0.43	0.57	−5.08
2006	0.60	0.64	−12.49	0.58	0.60	−10.84	0.51	0.53	−10.63	0.59	0.59	−5.30
2007	0.56	0.58	4.49	0.58	0.60	4.86	0.40	0.42	12.25	0.37	0.39	11.88
2008	0.59	0.63	9.46	0.60	0.63	10.54	0.59	0.64	10.57	0.59	0.67	14.31
2009	0.40	0.41	5.66	0.41	0.43	9.42	0.38	0.39	7.96	0.39	0.41	6.42
2010	0.47	0.56	26.25	0.48	0.60	28.17	0.52	0.59	23.76	0.41	0.50	27.29
2011	0.71	0.75	14.78	0.74	0.79	16.33	0.64	0.66	14.33	0.58	0.60	17.03
2012	0.43	0.43	1.55	0.47	0.47	3.71	0.09	0.21	−2.77	0.24	0.29	0.64
2013	0.64	0.66	9.53	0.66	0.69	11.52	0.52	0.54	6.68	0.40	0.44	11.83
2014	0.53	0.56	5.06	0.55	0.58	7.19	0.35	0.38	13.45	0.34	0.36	9.10

Overall, applying the LS method improved agreement between observed and simulated streamflows using the bias-corrected SPPs. In addition, the corrected SPP estimates better represented the temporal variability of simulated runoff. However, CEQUEAU performance varied across products, with better results from IMERG-Late and IMERG-Early, whereas PERSIANN-CCS and PDIR-Now showed more limited performance (Figure 9).

For the entire calibration period, the NSE values for the SPPs ranged from 0.45 to 0.55, with IMERG-Late showing the best performance (NSE = 0.55, Figure 9b), followed by IMERG-Early (NSE = 0.53, Figure 9a). These values, together with R^2 values ranging from 0.55 to 0.59 and PBIAS values below 4%, indicate good overall agreement between observed and simulated streamflows during the calibration period. In contrast, PERSIANN-CCS and PDIR-Now showed lower agreement (NSE $\leq$ 0.48), indicating a lower consistency in reproducing the observed streamflow dynamics (Figure 9c,d).

For the entire validation period, the overall performance of the IMERG products remained relatively stable, with NSE values between 0.53 and 0.56 and R^2 values close to 0.55, indicating adequate predictive capability after calibration. In contrast, PERSIANN-CCS and PDIR-Now experienced a more pronounced decline in performance (NSE $\leq$ 0.33), suggesting lower temporal consistency in the simulated streamflow series. Overall PBIAS values for the four SPPs remained within $\pm$8%, indicating that bias correction reduced systematic errors propagated from precipitation estimates to simulated streamflows, although some deviations remained. Overall, these results indicate that bias correction substantially improved the suitability of the SPPs for hydrological simulations.

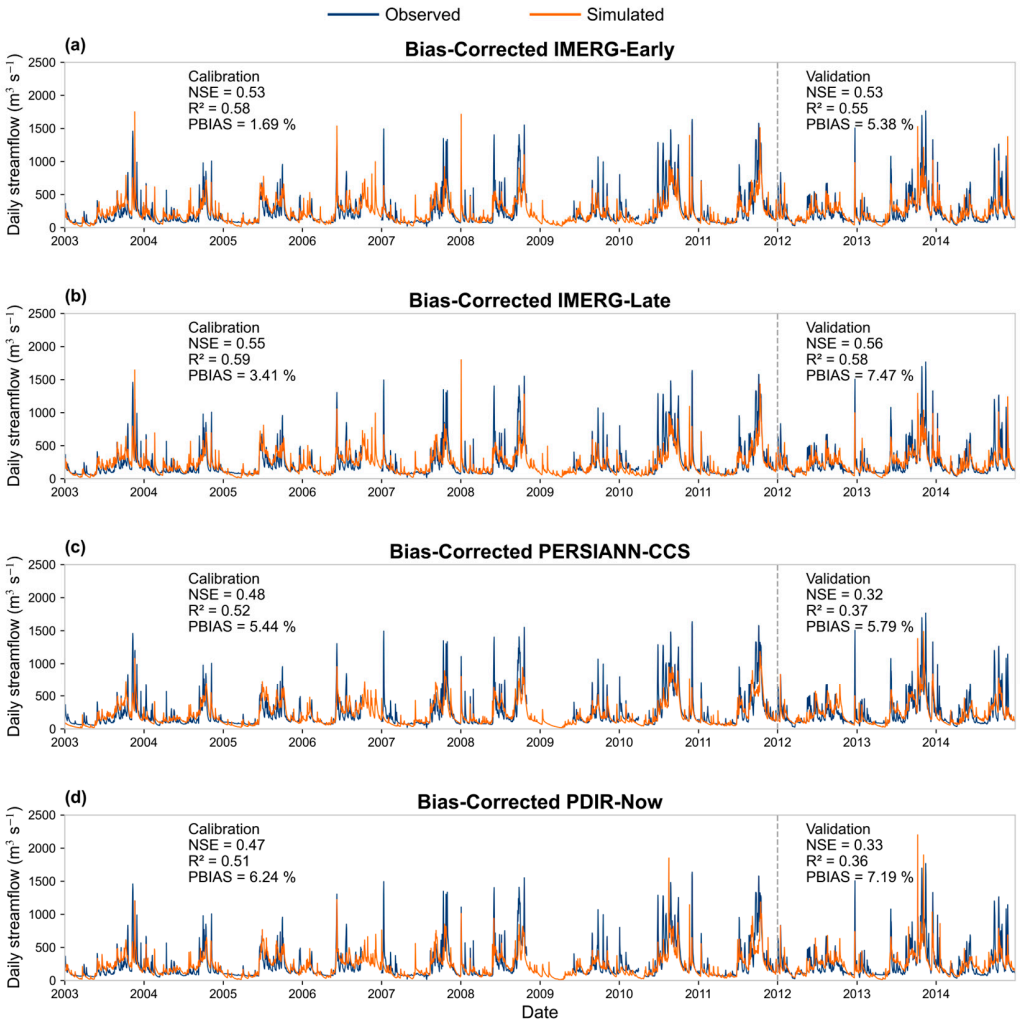


Figure 9. Hydrographs of observed and simulated daily streamflows using LS-corrected SPP estimates during the calibration (2003–2011) and validation (2012–2014) periods: (**a**) Bias-Corrected IMERG-Early, (**b**) Bias-Corrected IMERG-Late, (**c**) Bias-Corrected PERSIANN-CCS, and (**d**) Bias-Corrected PDIR-Now. The vertical dashed line indicates the transition between the calibration (2003–2011) and validation (2012–2014) periods.

Figure 10 presents the interannual hydrograph of observed and simulated daily streamflows using the SPPs. A considerable difference is evident between the streamflows simulated with IMERG-Early and the observed streamflows. From September to March, the model substantially underestimated streamflows. Although agreement improved slightly in April and May, the IMERG-Early estimates still failed to reproduce the observed streamflows adequately. The statistical criteria support this result: the negative NSE indicates unsatisfactory performance, while the positive PBIAS reveals a clear tendency toward

underestimation. Although the R^2 value indicates that the model explains more than half of the observed variability, this level of agreement is insufficient to represent streamflow dynamics reliably.

IMERG-Late exhibited behavior similar to IMERG-Early, underestimating most months except July. Furthermore, during periods of maximum streamflow, the model tended to underestimate peak flows. This general tendency toward underestimation is also reflected in the positive PBIAS value (42.01%), which was higher than that obtained for IMERG-Early. An NSE value of −0.01 confirms that the model performed poorly and could not reproduce the observed streamflows adequately. Although IMERG-Late has a longer latency period (12 h) and incorporates information from additional satellite sources, its overall behavior was very similar to that of IMERG-Early.

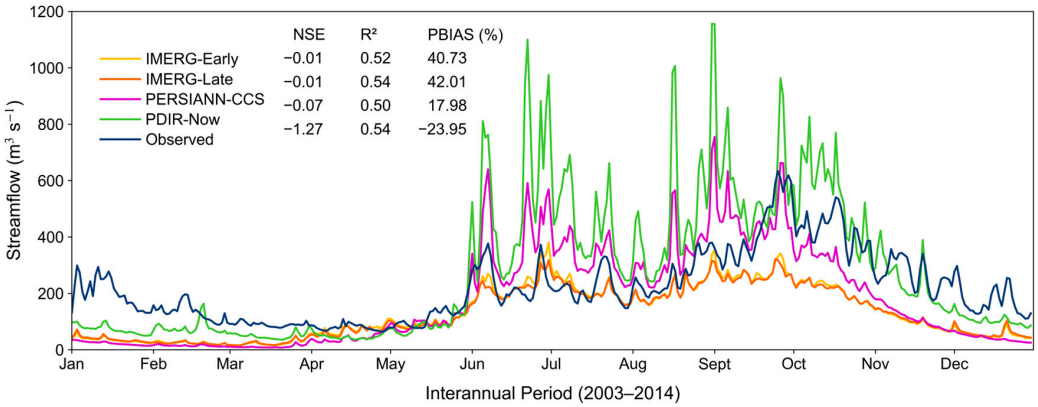


Figure 10. Interannual hydrographs of observed and simulated daily streamflows using original SPP estimates during 2003–2014.

For PDIR-Now, the model substantially overestimated streamflow from June to October. Consistent with this general overestimation, PBIAS was strongly negative (−23.95%). The simulated streamflows showed better agreement during the low-flow season (March to May). However, the negative NSE indicates that the model could not adequately reproduce the observed streamflows. For PERSIANN-CCS, although the NSE value was closer to zero, its performance remained unsatisfactory according to the criteria proposed by Moriasi et al. [62]. This result indicates that the model had limited skill in reproducing observed streamflows and that PERSIANN-CCS estimates were ineffective at simulating mean daily streamflows in the TRB. Furthermore, the positive PBIAS value indicates a general tendency toward underestimation during most months (October to April), although overestimation was also observed between June and August.

Figure 11 presents the interannual hydrographs of simulated streamflow from the four SPPs after bias correction using the LS method. Graphically, both IMERG products exhibit similar behavior: the streamflows simulated with the corrected SPPs closely match observed streamflows in both the wet and dry seasons and reproduce peak flows during flood periods. Similarly, streamflows simulated with the corrected PDIR-Now product showed improved agreement with observed streamflows compared with those obtained using the original estimates. However, some peaks were overestimated during August and September. In contrast, the corrected PERSIANN-CCS product exhibits more noticeable discrepancies during the first months of the year and during the October peak flows. Overall, during the dry season, streamflows simulated with all corrected SPPs were closer to the observed values.

The LS correction primarily reduces systematic bias in precipitation estimates, making mean monthly accumulations more consistent with observed values. Bias correction using the LS method substantially improved SPP performance. The IMERG products were

the most successful in reproducing both the magnitude and seasonality of the observed streamflows. However, some limitations remain, such as the overestimation of certain peak flows (June, August, October, and November), indicating that the LS method does not eliminate all sources of bias.

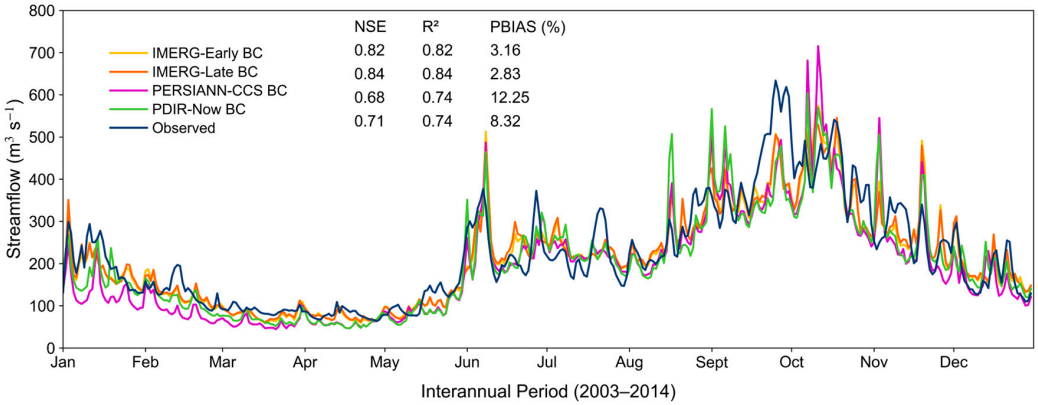


Figure 11. Interannual hydrographs of observed and simulated daily streamflows using LS-corrected SPP estimates during 2003–2014.

5. Discussion

5.1. Analysis of SPP Performance for Precipitation Estimation

This study analyzed the performance of four near-real-time SPPs for estimating monthly precipitation in the TRB. IMERG-Early and IMERG-Late performed better than PERSIANN-CCS and PDIR-Now, achieving higher correlations and positive NSE values. IMERG-Late performed slightly better, with a bias closer to zero. However, both products tended to underestimate precipitation during several months, especially during the rainy season. This behavior is consistent with Li et al. [28] in a subtropical region of southern China, where IMERG-Early and IMERG-Late also tended to underestimate precipitation, although to a lesser extent. Similarly, Jiang et al. [22] found that both products underestimated precipitation during high-intensity events in southern China. These findings suggest that, although IMERG products generally perform well, they may have limitations in estimating precipitation magnitude during extreme events and periods of abundant rainfall.

In our study, PERSIANN-CCS and PDIR-Now showed greater limitations in estimating precipitation. PERSIANN-CCS had the lowest correlation, negative NSE values, and a tendency to underestimate precipitation during the dry season and overestimate it during the rainy season. In turn, PDIR-Now presented the highest MAE and bias, with a pronounced overestimation during the rainy season. Justo et al. [63], in Brazil, found similar behavior: PERSIANN-CCS and PDIR-Now overestimated precipitation during the rainy season, whereas during the dry season both SPPs showed more pronounced underestimations. These findings are consistent with behavior observed in the TRB, particularly PDIR-Now's overestimation during the rainy season [64]. Gunathilake et al. [16] identified limitations in PERSIANN-CCS and PDIR-Now for adequately representing precipitation, particularly during extreme events. Furthermore, they noted that the quality of estimated precipitation is a key determinant of streamflow simulation performance.

5.2. Analysis of Streamflow Simulation

The use of SPPs in hydrological modeling has become increasingly common [65–70], as they provide extensive spatial coverage and greater data availability compared with observations from meteorological stations. In our study of the TRB, the original estimates from the four near-real-time SPPs performed poorly in streamflow simulation. The hydro-

graphs generated using the four SPPs did not adequately match the observed hydrograph. They yielded NSE values below 0.18, showing a limited ability to represent the basin's hydrological dynamics. Simulations using observed precipitation data yielded NSE values close to 0.70 in both calibration and validation; conversely, streamflows simulated using the original SPPs did not align well with observed flows, demonstrating how satellite precipitation errors propagate into hydrological modeling. Following bias correction via LS, NSE values exceeded 0.50 for the IMERG products, indicating that the reduction in systematic errors improved hydrological performance. Thus, the results highlight the importance of precipitation input quality in hydrological modeling, as differences in model performance were associated with precipitation dataset quality.

Several studies in different regions have reported limitations in using near-real-time SPPs for streamflow simulation. Dou et al. [71] reported unsatisfactory performance of products such as IMERG-Early, IMERG-Late, and PERSIANN-CCS in northwestern China, with NSE values close to zero and a tendency to underestimate streamflow. Jiang et al. [22] also analyzed IMERG-Early and IMERG-Late in China and reported both underestimations and overestimations in daily streamflow simulations. Meanwhile, Tan et al. [72] found in Kelantan (northeastern Peninsular Malaysia) that IMERG-Early and IMERG-Late underestimated daily streamflow and showed limitations at reproducing peak flows, which are relevant for hydrological risk management. These results are consistent with those obtained in the present study for the TRB, where IMERG-Early and IMERG-Late showed similar behavior, characterized mainly by streamflow underestimation.

Regarding PERSIANN-CCS and PDIR-Now, Salehi et al. [73] reported in California (United States) that PDIR-Now exhibited intermittent behavior, whereas PERSIANN-CCS tended to underestimate runoff. This is consistent with Ndemere et al. [17] in Zimbabwe, where PERSIANN-CCS underestimated streamflow during both the calibration and validation periods; however, they also reported that PDIR-Now underestimated streamflow during both periods. In the TRB, PERSIANN-CCS and PDIR-Now showed both overestimations and underestimations of streamflow and generated pronounced peaks during the rainy season, particularly PDIR-Now. These differences demonstrate that the hydrological performance of SPPs depends not only on their estimation algorithms but also on local precipitation regimes and the hydrological characteristics of each basin.

The TRB is characterized by orographic and convective precipitation, short-duration intense storms, and complex topography dominated by mountainous terrain and dense tropical vegetation. In contrast, other basins commonly exhibit more continuous and less intense precipitation regimes. These differences indicate that SPP accuracy is strongly influenced by precipitation type and terrain complexity; therefore, performance may vary across regions. Previous studies conducted in the United States [13], Sri Lanka [16], Türkiye [74], and China [75] have also reported limitations of SPPs for streamflow simulation; our findings suggest that these limitations may be more pronounced in tropical regions defined by high spatial and temporal variability in precipitation. The better performance obtained using observed precipitation than using the four uncorrected SPPs indicates that the quality of the precipitation input data was a major factor contributing to differences in hydrological performance. CEQUEAU has demonstrated its ability to reproduce basin hydrological responses in Mexico [53,54] and Colombia [76] with characteristics similar to those of the TRB, indicating that the discrepancies primarily originate from the SPP estimates.

Therefore, the results highlight the importance of bias correction before using these SPPs in hydrological simulations. In our study, we applied the LS method for bias correction, resulting in improved streamflow simulations for all four corrected SPPs and confirming its effectiveness in reducing systematic errors. Previous studies [42,77,78] have also reported improvements following its application, supporting its use in hydrological modeling.

Nevertheless, the results indicate that the LS method alone is insufficient to adequately represent extreme-event variability.

Although the LS method improved SPP performance in the TRB, the simulations still showed underestimations and overestimations of peak flows, indicating that reducing systematic bias alone was insufficient to reproduce the variability associated with extreme precipitation events. Because the TRB experiences prolonged dry periods followed by intense storms, future studies should evaluate more advanced bias-correction techniques to better represent extreme precipitation events and their resulting hydrological response.

5.3. Limitations and Future Research

The distributed hydrological model CEQUEAU was used to simulate streamflow in the TRB. CEQUEAU uses precipitation values assigned to specific input points rather than working directly with pixels from the SPPs. Precipitation estimates from the SPPs were extracted solely at the 35 locations corresponding to meteorological stations. Consequently, these products' spatial coverage was not fully utilized; precipitation variability in areas distant from the stations, particularly in the basin's mountainous sectors, may not have been fully represented. In light of this, future work involving CEQUEAU would benefit from the following:

- Employing a denser network of input points, including locations where no meteorological stations exist.
- Analyzing the effect of resampling the SPPs to a common resolution or to the grid used by CEQUEAU, given that they retained their original spatial resolutions in this study.
- Since the CEQUEAU evaluation focused on daily streamflow, it would be valuable to analyze shorter time scales to study intense rainfall events and flash floods.

The near-real-time SPPs used in this study become available just hours after the precipitation occurs, making them particularly useful for operational applications. However, unlike final-version precipitation products, released days or even months later and adjusted using ground-based measurements or other data sources, near-real-time products entail greater uncertainty. Therefore, evaluating their performance at the local scale is essential before applying them to hydrological modeling. In this study, the Linear Scaling (LS) method was used to correct SPP bias because of its low computational cost, ease of implementation, and satisfactory performance reported in numerous studies. Applying this method improved the SPP precipitation estimates used as input for streamflow simulations. However, it would be advisable to evaluate other bias-correction methods at daily time steps, such as non-linear and machine learning approaches, particularly to represent extreme events better.

6. Conclusions

Near-real-time SPPs are available only a few hours after observation, before incorporating all the information sources used for their correction, which may reduce their accuracy. However, their immediate availability makes them a valuable alternative for operational hydrological applications. Therefore, evaluating their ability to simulate daily streamflow in the TRB is essential to determine their reliability and potential for hydrological monitoring, water resources management, and flood early warning systems. This study evaluated the performance of four near-real-time SPPs (IMERG-Early, IMERG-Late, PERSIANN-CCS, and PDIR-Now) for simulating daily streamflow in the TRB using the CEQUEAU hydrological model. We first assessed the performance of the SPPs by comparing their estimates with observed precipitation data from meteorological stations, then evaluated their performance in hydrological simulations. In addition, we applied the Linear Scaling (LS) method to correct biases in the SPP estimates.

The main findings show that, at the monthly scale, IMERG-Early and IMERG-Late generally tended to underestimate precipitation, whereas PDIR-Now showed a pronounced tendency to overestimate it. PERSIANN-CCS showed greater variability in its precipitation estimates and the lowest overall agreement with observed precipitation. These biases were also reflected in the hydrological simulations. IMERG-Early and IMERG-Late showed similar behavior, with both underestimating the daily streamflow observed at the hydrometric station and yielding unsatisfactory NSE values for all analyzed years. For PDIR-Now, the model did not adequately reproduce daily streamflow, with substantial overestimation of several peak flows during the rainy season. For PERSIANN-CCS, although the simulated peaks were less pronounced, overall performance remained unsatisfactory. These results highlight the importance of evaluating SPP performance before using their estimates as input data for hydrological models in tropical regions such as the TRB.

Bias correction of the SPPs using the LS method improved hydrological simulations in the TRB. This improvement was particularly evident for IMERG-Early and IMERG-Late, which, after bias correction, achieved acceptable NSE values in most years and PBIAS values ranging from satisfactory to very good according to the criteria proposed by Moriasi et al. [62]. Improvements were also observed for the PERSIANN products, although their NSE values remained lower than those obtained with IMERG. Therefore, although the LS method is relatively simple to implement, it improved the suitability of SPP estimates for hydrological simulation, as streamflows simulated using bias-corrected precipitation estimates showed greater agreement with observed streamflows.

Hydrological simulations using observed precipitation showed that the CEQUEAU model adequately represented daily streamflow in the TRB during both calibration and validation. Although the model tended to underestimate streamflow in most years, most PBIAS values were classified as good to very good according to Moriasi et al. [62], supporting the use of simulations based on observed precipitation as a reference for evaluating simulations driven by SPP estimates.

The results of this study demonstrate that the rapid availability of near-real-time SPP data does not necessarily ensure reliable hydrological simulations, highlighting the importance of evaluating and, when necessary, correcting systematic biases before their application in hydrological modeling. In this study, applying the LS method improved the performance of SPP estimates in streamflow simulations. However, residual errors in the representation of peak flows indicate that reducing systematic bias alone may be insufficient to fully reproduce hydrological variability in the TRB. Finally, these findings may serve as a reference for other regions with similar characteristics, particularly those where observed precipitation data are limited.

Author Contributions: Conceptualization, L.C.-H., K.M.B., F.M.-H., M.A.G.-A., G.P.M.-R. and C.A.M.-L.; methodology, L.C.-H., K.M.B. and F.M.-H.; formal analysis, L.C.-H., K.M.B., F.M.-H. and M.A.G.-A.; investigation, L.C.-H., K.M.B., F.M.-H., M.A.G.-A., G.P.M.-R. and C.A.M.-L.; resources, L.C.-H., F.M.-H. and C.E.T.-A.; data curation, L.C.-H., K.M.B. and F.M.-H.; writing—original draft preparation, L.C.-H., K.M.B., F.M.-H. and C.E.T.-A.; writing—review and editing, L.C.-H., K.M.B., F.M.-H., G.P.M.-R. and C.A.M.-L.; supervision, L.C.-H., K.M.B., F.M.-H., M.A.G.-A., G.P.M.-R. and C.A.M.-L.; project administration, L.C.-H., K.M.B. and F.M.-H.; funding acquisition, L.C.-H., K.M.B. and F.M.-H. All authors have read and agreed to the published version of the manuscript.

Funding: This research received no external funding.

Data Availability Statement: Data are contained within the article.

Acknowledgments: The authors gratefully acknowledge the Secretaría de Ciencia, Humanidades, Tecnología e Innovación (SECIHTI) for the master's scholarship awarded to the first author. The authors also gratefully acknowledge the Comisión Nacional del Agua, CONAGUA), through its

Sistema de Información Hidrológica (SIH) (https://sih.conagua.gob.mx/, accessed on 12 October 2025), the NASA Goddard Earth Sciences Data and Information Services Center (GES DISC) (https://disc.gsfc.nasa.gov/, accessed on 20 September 2025) for providing the IMERG datasets, and the Center for Hydrometeorology and Remote Sensing (https://chrsdata.eng.uci.edu/, accessed on 20 September 2025) for providing the PERSIANN datasets.

Conflicts of Interest: The authors declare no conflicts of interest.

References

1. Behrangi, A.; Khakbaz, B.; Jaw, T.C.; AghaKouchak, A.; Hsu, K.; Sorooshian, S. Hydrologic evaluation of satellite precipitation products over a mid-size basin. *J. Hydrol.* **2011**, *397*, 225–237. [CrossRef]
2. Magaña-Hernández, F.; Bâ, K.M.; Guerra-Cobián, V.H. Estimación del hidrograma de crecientes con modelación determinística y precipitación derivada de radar. *Agrociencia* **2013**, *47*, 739–752.
3. Joyce, R.J.; Janowiak, J.E.; Arkin, P.A.; Xie, P. CMORPH: A method that produces global precipitation estimates from passive microwave and infrared data at high spatial and temporal resolution. *J. Hydrometeorol.* **2004**, *5*, 487–503. [CrossRef]
4. Funk, C.; Peterson, P.; Landsfeld, M.; Pedreros, D.; Verdin, J.; Rowland, J.; Romero, B.; Husak, G.; Michaelsen, J.; Verdin, A. A quasi-global precipitation time series for drought monitoring. *U.S. Geol. Surv. Data Ser.* **2014**, *832*, 4. [CrossRef]
5. Herman, A.; Kumar, V.B.; Arkin, P.A.; Kousky, J.V. Objectively determined 10-day African rainfall estimates created for famine early warning systems. *Int. J. Remote Sens.* **1997**, *18*, 2147–2159. [CrossRef]
6. Huffman, G.J.; Adler, R.F.; Bolvin, D.T.; Gu, G.; Nelkin, E.J.; Bowman, K.P.; Hong, Y.; Stocker, E.F.; Wolff, D.B. The TRMM Multisatellite Precipitation Analysis (TMPA): Quasi-global, multiyear, combined-sensor precipitation estimates at fine scales. *J. Hydrometeorol.* **2007**, *8*, 38–55. [CrossRef]
7. Okamoto, K.; Ushio, T.; Iguchi, T.; Takahashi, N.; Iwanami, K. The Global Satellite Mapping of Precipitation (GSMaP) project. In Proceedings of the IEEE International Geoscience and Remote Sensing Symposium (IGARSS), Seoul, Republic of Korea, 29 July 2005; Volume 5, pp. 3414–3416. [CrossRef]
8. Sorooshian, S.; Hsu, K.L.; Gao, X.; Gupta, H.V.; Imam, B.; Braithwaite, D. Evaluation of PERSIANN system satellite-based estimates of tropical rainfall. *Bull. Am. Meteorol. Soc.* **2000**, *81*, 2035–2046. [CrossRef]
9. Hou, A.Y.; Kakar, R.K.; Neeck, S.; Azarbarzin, A.A.; Kummerow, C.D.; Kojima, M.; Oki, R.; Nakamura, K.; Iguchi, T. The Global Precipitation Measurement mission. *Bull. Am. Meteorol. Soc.* **2014**, *95*, 701–722. [CrossRef]
10. Jiang, S.; Liu, S.; Ren, L.; Yong, B.; Zhang, L.; Wang, M.; Lu, Y.; He, Y. Hydrologic evaluation of six high resolution satellite precipitation products in capturing extreme precipitation and streamflow over a medium-sized basin in China. *Water* **2017**, *10*, 25. [CrossRef]
11. Khoshchehreh, M.; Ghomeshi, M.; Shahbazi, A. Hydrological evaluation of global gridded precipitation datasets in a heterogeneous and data-scarce basin in Iran. *J. Earth Syst. Sci.* **2020**, *129*, 201. [CrossRef]
12. Li, J.; Yuan, D.; Ma, M.; Liu, J. Simulation of Karst Floods with a Hydrological Model Improved by Meteorological Model Coupling. *J. Hydrometeorol.* **2022**, *23*, 185–207. [CrossRef]
13. Ray, R.L.; Sishodia, R.P.; Tefera, G.W. Evaluation of Gridded Precipitation Data for Hydrologic Modeling in North-Central Texas. *Remote Sens.* **2022**, *14*, 3860. [CrossRef]
14. Uysal, G. Product- and Hydro-Validation of Satellite-Based Precipitation Data Sets for a Poorly Gauged Snow-Fed Basin in Turkey. *Water* **2022**, *14*, 2758. [CrossRef]
15. Yaswanth, P.; Kannan, B.A.M.; Bindhu, V.M.; Balaji, C.; Narasimhan, B. Evaluation of Remote Sensing Rainfall Products, Bias Correction and Temporal Disaggregation Approaches, for Improved Accuracy in Hydrologic Simulations. *Water Resour. Manag.* **2023**, *37*, 3069–3092. [CrossRef]
16. Gunathilake, M.B.; Senerath, T.; Rathnayake, U. Artificial neural network based PERSIANN data sets in evaluation of hydrologic utility of precipitation estimations in a tropical watershed of Sri Lanka. *AIMS Geosci.* **2021**, *7*, 478–489. [CrossRef]
17. Ndemere, K.; Gumindoga, W.; Makurira, H.; Rwasoka, D.T. Performance evaluation of multiple satellite rainfall products in mountainous catchment of Eastern Zimbabwe. *Sci. Afr.* **2024**, *23*, e02120. [CrossRef]
18. Bertini, C.; Buonora, L.; Moccia, B. Performance of satellite-based rainfall observations for hydrological modelling in ungauged areas. *AIP Conf. Proc.* **2025**, *3315*, 400039. [CrossRef]
19. Eini, M.R.; Rahmati, A.; Piniewski, M. Hydrological application and accuracy evaluation of PERSIANN satellite-based precipitation estimates over a humid continental climate catchment. *J. Hydrol. Reg. Stud.* **2022**, *41*, 101109. [CrossRef]
20. Cao, D.; Li, H.; Hou, E.; Song, S.; Lai, C. Assessment and Hydrological Validation of Merged Near-Real-Time Satellite Precipitation Estimates Based on the Gauge-Free Triple Collocation Approach. *Remote Sens.* **2022**, *14*, 3835. [CrossRef]

21. Jiang, S.; Ren, L.; Xu, C.Y.; Yong, B.; Yuan, F.; Liu, Y.; Yang, X.; Zeng, X. Statistical and hydrological evaluation of the latest Integrated Multi-satellitE Retrievals for GPM (IMERG) over a midlatitude humid basin in South China. *Atmos. Res.* **2018**, *214*, 418–429. [CrossRef]
22. Jiang, S.; Ding, Y.; Liu, R.; Wei, L.; Liu, Y.; Ren, M.; Ren, L. Assessing the Potential of IMERG and TMPA Satellite Precipitation Products for Flood Simulations and Frequency Analyses over a Typical Humid Basin in South China. *Remote Sens.* **2022**, *14*, 4406. [CrossRef]
23. Pourentezari, S.; Salehi, H.; Haghighi, A.R.; Sadeghi, M.; Faridhosseini, A. Towards Accurate Flood Forecasting: Integrating Satellite Data, Hydrological Modeling, and Deep Learning. *J. Flood Risk Manag.* **2025**, *18*, e70155. [CrossRef]
24. Saouabe, T.; El Khalki, E.M.; Saidi, M.E.M.; Najmi, A.; Hadri, A.; Rachidi, S.; Jadoud, M.; Tramblay, Y. Evaluation of the GPM-IMERG Precipitation Product for Flood Modeling in a Semi-Arid Mountainous Basin in Morocco. *Water* **2020**, *12*, 2516. [CrossRef]
25. Gautam, J.; O, S.; Vinod, D.; Mahesha, A. Evaluation of GPM IMERG satellite precipitation for rainfall–runoff modelling in Great Britain. *Hydrol. Sci. J.* **2024**, *69*, 2010–2025. [CrossRef]
26. Guragain, S.; Shah, S.; Albano, R.; Kim, S.; Hammad, M.; Asif, M. Quantifying the Added Values of a Merged Precipitation Product in Streamflow Prediction over the Central Himalayas. *Remote Sens.* **2025**, *17*, 2170. [CrossRef]
27. Syakira, N.; Tan, M.L.; Zulkafli, Z.; Zhang, F.; Tangang, F.; Chang, C.K.; Ibrahim, W.M.M.W.; Ramli, M.H.P. Assessment of Three GPM IMERG Products for GIS-Based Tropical Flood Hazard Mapping Using Analytical Hierarchy Process. *Water* **2023**, *15*, 2195. [CrossRef]
28. Li, X.; Chen, Y.; Deng, X.; Zhang, Y.; Chen, L. Evaluation and Hydrological Utility of the GPM IMERG Precipitation Products over the Xinfengjiang River Reservoir Basin, China. *Remote Sens.* **2021**, *13*, 866. [CrossRef]
29. Yan, Y.; Wang, G.; Nanding, N.; Chen, W. Hydrological Evaluation of Satellite-Based Precipitation Products in Hunan Province. *Remote Sens.* **2022**, *14*, 3127. [CrossRef]
30. Atiah, W.A.; Johnson, R.; Muthoni, F.K.; Mengistu, G.T.; Amekudzi, L.K.; Kwabena, O.; Kizito, F. Bias correction and spatial disaggregation of satellite-based data for the detection of rainfall seasonality indices. *Heliyon* **2023**, *9*, e17604. [CrossRef]
31. Omondi, C.K.; Rientjes, T.H.M.; Booij, M.J.; Nelson, A.D. Satellite rainfall bias correction incorporating effects on simulated crop water requirements. *Int. J. Remote Sens.* **2024**, *45*, 2269–2288. [CrossRef]
32. Rajesh, G.M.; Prasad, S.; Singh, S.K.; Al-Ansari, N.; Salem, A.; Mattar, M.A. Bias Correction of Satellite-Derived Climatic Datasets for Water Balance Estimation. *Water* **2025**, *17*, 2626. [CrossRef]
33. Ye, J.; Lu, Y.; Yang, X.; He, Z.; Huang, P.; Zheng, X. Bias Correction of Hourly Satellite Precipitation Products and Their Application in Hydrological Modeling in a Hilly Watershed, China. *Water* **2024**, *16*, 49. [CrossRef]
34. Dao, V.; Arellano, C.J.; Nguyen, P.; Almutlaq, F.; Hsu, K.; Sorooshian, S. Bias correction of satellite precipitation estimation using deep neural networks and topographic information over the Western U.S. *J. Geophys. Res. Atmos.* **2025**, *130*, e2024JD042181. [CrossRef]
35. Mashuri; Karlina; Sujono, J. Assessment of satellite-based rainfall products for drought monitoring in the Siak Watershed, Indonesia. *Environ. Chall.* **2025**, *19*, 101134. [CrossRef]
36. Londhe, D.S.; Katpatal, Y.B.; Bokde, N.D. Performance Assessment of Bias Correction Methods for Precipitation and Temperature from CMIP5 Model Simulation. *Appl. Sci.* **2023**, *13*, 9142. [CrossRef]
37. Beyene, T.L.; Haile, A.T.; Goshime, D.W.; Birhan, T.S. Comparison of bias correction methods to enhance CHIRP rainfall estimates for improved streamflow simulation at Ziway-Shalla catchment, Ethiopia. *J. Hydrol. Reg. Stud.* **2025**, *62*, 102920. [CrossRef]
38. Gado, T.A.; Zamzam, D.H.; Guo, Y.; Zeidan, B.A. Evaluation of satellite-based rainfall estimates in the upper Blue Nile basin. *J. Earth Syst. Sci.* **2024**, *133*, 27. [CrossRef]
39. Andari, R.; Nurhamidah, N.; Daoed, D.; Marzuki. Evaluation of bias correction methods for multi-satellite rainfall estimation products. *IOP Conf. Ser. Earth Environ. Sci.* **2024**, *1317*, 012008. [CrossRef]
40. Zahrani, N.; Suhartanto, E.; Andawayanti, U. Assessment of Bias-Correction Methods for CHIRPS Satellite Rainfall Estimates in the Petung Watershed, Indonesia. *J. Penelit. Pendidik. IPA* **2025**, *11*, 43–51. [CrossRef]
41. Ferynandari, A.M.; Suhartanto, E.; Prasetyorini, L. Evaluasi kinerja teknik koreksi bias untuk meningkatkan akurasi Global Precipitation Measurement (GPM) di daerah aliran sungai Rejoso, Indonesia. *J. Penelit. Pengelolaan Drh. Aliran Sungai* **2025**, *9*, 165–180. [CrossRef]
42. Soo, E.Z.X.; Jaafar, W.Z.W.; Lai, S.H.; Othman, F.; Elshafie, A.; Islam, T.; Srivastava, P.; Hadi, H.S.O. Precision of raw and bias-adjusted satellite precipitation estimations (TRMM, IMERG, CMORPH, and PERSIANN) over extreme flood events: Case study in Langat River Basin, Malaysia. *J. Water Clim. Chang.* **2020**, *11*, 322–342. [CrossRef]
43. Adem, E.; Elfeki, A.; Chaabani, A.; Alwegdani, A.; Hussain, S.; Elhag, M. Impact of satellite precipitation estimation methods on the hydrological response: Case study Wadi Nu'man basin, Saudi Arabia. *Theor. Appl. Climatol.* **2024**, *155*, 3907–3925. [CrossRef]
44. Elsebaie, I.H.; Kawara, A.Q.; Alharbi, R.; Alnahit, A.O. Bias Correction Methods Applied to Satellite Rainfall Products over the Western Part of Saudi Arabia. *Atmosphere* **2025**, *16*, 772. [CrossRef]

45. Bodjrènou, M.; Peng, K.; Affèwé, D.J.; Hounkpè, J.; Donnou, H.E.V.; Adounkpè, J.; Akpo, A.B. Assessment of Satellite-Based Rainfall Products for Flood Modeling in the Ouémé River Basin in Benin (West Africa). *Hydrology* **2025**, *12*, 71. [CrossRef]
46. Zhang, M.; Cheng, Y.; Ning, S.; Zhou, Y.; Wu, C.; Cui, Y.; Jin, J.; Thapa, B.R. Multi-source precipitation fusion for hydrological models: Correction and metrics importance analysis. *J. Hydrol. Reg. Stud.* **2026**, *64*, 103291. [CrossRef]
47. Huffman, G.J.; Bolvin, D.T.; Braithwaite, D.; Hsu, K.L.; Joyce, R.J.; Kidd, C.; Nelkin, E.J.; Sorooshian, S.; Stocker, E.F.; Tan, J.; et al. Integrated Multi-satellite Retrievals for the Global Precipitation Measurement (GPM) mission (IMERG). In *Satellite Precipitation Measurement: Volume 1 (Advances in Global Change Research)*; Levizzani, V., Kidd, C., Kirschbaum, D., Kummerow, C., Nakamura, K., Turk, F.J., Eds.; Springer: Cham, Switzerland, 2020; Volume 67, pp. 343–353. [CrossRef]
48. Nguyen, P.; Ombadi, M.; Gorooh, V.A.; Shearer, E.J.; Sadeghi, M.; Sorooshian, S.; Hsu, K.; Bolvin, D.; Ralph, M.F. PERSIANN Dynamic Infrared–Rain Rate (PDIR-Now): A near-real-time, quasi-global satellite precipitation dataset. *J. Hydrometeorol.* **2020**, *21*, 2893–2906. [CrossRef]
49. Hong, Y.; Hsu, K.L.; Sorooshian, S.; Gao, X. Precipitation estimation from remotely sensed imagery using an artificial neural network cloud classification system. *J. Appl. Meteorol.* **2004**, *43*, 1834–1852. [CrossRef]
50. Jarvis, A.; Reuter, H.I.; Nelson, A.; Guevara, E. *Hole-Filled Seamless SRTM Data V4*; International Centre for Tropical Agriculture (CIAT): Palmira, Colombia, 2008. Available online: https://srtm.csi.cgiar.org (accessed on 30 November 2025).
51. Morin, G.; Sochanski, W.; Paquet, P. *Le Modèle de Simulation de Quantité CEQUEAU-ONU: Manuel de Référence*; Rapport de recherche No. 519; Organisation des Nations Unies et INRS-Eau: Sainte-Foy, QC, Canada, 1998.
52. Magaña-Hernández, F. Estimación de Caudales Máximos a Partir de Modelos Hidrológicos Con Datos de Precipitación de Percepción Remota. Ph.D. Thesis, Universidad Autónoma del Estado de México, Toluca, Mexico, 2014.
53. Magaña Hernández, F.; Mora Ortiz, R.S.; Quiroga, L.A.; Martínez Jiménez, J.C.; Munguía Balvanera, E. Simulación hidrológica de la cuenca del río Teapa. *Rev. Espac. I+D Innov. Más Desarro.* **2023**, *12*, 89–104. [CrossRef]
54. Magaña-Hernández, F.; Muñoz-Gómez, A.C.; Mora-Ortiz, R.S.; Quiroga, L.A.; Guerra-Cobián, V.H. Estimación de caudales en cuencas no aforadas por el modelo hidrológico CEQUEAU. *Agrociencia* **2021**, *55*, 99–115. [CrossRef]
55. Morin, G. CEQUEAU hydrological model. In *Mathematical Models of Large Watershed Hydrology*; Singh, V.P., Frevert, D., Eds.; Water Resources Publications: Highlands Ranch, CO, USA, 2002; pp. 507–576.
56. Benesty, J.; Chen, J.; Huang, Y.; Cohen, I. Pearson correlation coefficient. In *Noise Reduction in Speech Processing (Springer Topics in Signal Processing)*; Haykin, S., Liu, K.R., Eds.; Springer: Berlin/Heidelberg, Germany, 2009; Volume 2, pp. 1–4. [CrossRef]
57. Willmott, C.J.; Matsuura, K. Advantages of the mean absolute error (MAE) over the root mean square error (RMSE) in assessing average model performance. *Clim. Res.* **2005**, *30*, 79–82. [CrossRef]
58. Nash, J.; Sutcliffe, J. River flow forecasting through conceptual models part I—A discussion of principles. *J. Hydrol.* **1970**, *10*, 282–290. [CrossRef]
59. Rivera, J.; Marianetti, G.; Hinrichs, S. Validation of CHIRPS precipitation dataset along the Central Andes of Argentina. *Atmos. Res.* **2018**, *213*, 437–449. [CrossRef]
60. Shrestha, M.; Acharya, S.C.; Shrestha, P.K. Bias correction of climate models for hydrological modelling–are simple methods still useful? *Meteorol. Appl.* **2017**, *24*, 531–539. [CrossRef]
61. Morin, G.; Paquet, P. *Modèle Hydrologique CEQUEAU*; Rapport de Recherche No. R000926; INRS-ETE: Québec, QC, Canada, 2007. Available online: https://espace.inrs.ca/id/eprint/1098/1/R000926.pdf (accessed on 24 July 2025).
62. Moriasi, D.N.; Gitau, M.W.; Pai, N.; Daggupati, P. Hydrologic and water quality models: Performance measures and evaluation criteria. *Trans. ASABE* **2015**, *58*, 17631785. [CrossRef]
63. Justo, L.A.J.; Gonçalves, C.L.; Polifke, F.; de Almeida França, J.R. Performance of PERSIANN satellite precipitation products in a complex-terrain environment: Rio de Janeiro, Brazil. *Theor. Appl. Climatol.* **2026**, *157*, 444. [CrossRef]
64. Ceferino-Hernández, L.; Magaña-Hernández, F.; Campos-Campos, E.; Morosanu, G.A.; Torres-Aguilar, C.E.; Mora-Ortiz, R.S.; Díaz, S.A. Assessment of PERSIANN Satellite Products over the Tulijá River Basin, Mexico. *Remote Sens.* **2024**, *16*, 2596. [CrossRef]
65. Bâ, K.M.; Balcázar, L.; Diaz, V.; Ortiz, F.; Gómez-Albores, M.A.; Díaz-Delgado, C. Hydrological Evaluation of PERSIANN-CDR Rainfall over Upper Senegal River and Bani River Basins. *Remote Sens.* **2018**, *10*, 1884. [CrossRef]
66. Tang, X.; Zhang, J.; Gao, C.; Ruben, G.B.; Wang, G. Assessing the uncertainties of four precipitation products for SWAT modeling in Mekong River Basin. *Remote Sens.* **2019**, *11*, 304. [CrossRef]
67. Tran, T.N.D.; Nguyen, B.Q.; Zhang, R.; Aryal, A.; Grodzka-Łukaszewska, M.; Sinicyn, G.; Lakshmi, V. Quantification of Gridded Precipitation Products for the Streamflow Simulation on the Mekong River Basin Using Rainfall Assessment Framework: A Case Study for the Srepok River Subbasin, Central Highland Vietnam. *Remote Sens.* **2023**, *15*, 1030. [CrossRef]
68. Gebremicael, T.G.; Deitch, M.J.; Gancel, H.N.; Croteau, A.C.; Haile, G.G.; Beyene, A.N.; Kumar, L. Satellite-based rainfall estimates evaluation using a parsimonious hydrological model in the complex climate and topography of the Nile River Catchments. *Atmos. Res.* **2022**, *266*, 105939. [CrossRef]
69. Liu, X.; Yang, T.; Hsu, K.; Liu, C.; Sorooshian, S. Evaluating the streamflow simulation capability of PERSIANN-CDR daily rainfall products in two river basins on the Tibetan Plateau. *Hydrol. Earth Syst. Sci.* **2017**, *21*, 169–181. [CrossRef]

70. Kabite Wedajo, G.; Kebede Muleta, M.; Gessesse Awoke, B. Performance evaluation of multiple satellite rainfall products for Dhidhessa River Basin (DRB), Ethiopia. *Atmos. Meas. Tech.* **2021**, *14*, 2299–2316. [CrossRef]
71. Dou, Y.; Ye, L.; Zhang, J.; Zhang, C.; Zhou, H. Evaluation of seven near-real-time satellite-based precipitation products for wet seasons in the Nierji Basin, China. *Remote Sens.* **2021**, *13*, 4552. [CrossRef]
72. Tan, M.L.; Samat, N.; Chan, N.W.; Roy, R. Hydro-meteorological assessment of three GPM satellite precipitation products in the Kelantan River Basin, Malaysia. *Remote Sens.* **2018**, *10*, 1011. [CrossRef]
73. Salehi, H.; Sadeghi, M.; Golian, S.; Nguyen, P.; Murphy, C.; Sorooshian, S. The Application of PERSIANN Family Datasets for Hydrological Modeling. *Remote Sens.* **2022**, *14*, 3675. [CrossRef]
74. Hafizi, H.; Sorman, A.A. Assessment of 13 Gridded Precipitation Datasets for Hydrological Modeling in a Mountainous Basin. *Atmosphere* **2022**, *13*, 143. [CrossRef]
75. Gao, Z.; Tang, G.; Jing, W.; Hou, Z.; Yang, J.; Sun, J. Evaluation of Multiple Satellite, Reanalysis, and Merged Precipitation Products for Hydrological Modeling in the Data-Scarce Tributaries of the Pearl River Basin, China. *Remote Sens.* **2023**, *15*, 5349. [CrossRef]
76. Piñeros Dueñas, K.N. Modelación Hidrológica con CEQUEAU y SWAT Para la Evaluación del Impacto del Uso/Cobertura del Suelo en el Caudal de la Cuenca del río Garagoa, Colombia. Master's Thesis, Universidad Autónoma del Estado de México, Toluca, Mexico, 2024.
77. Tumsa, B.C. Performance assessment of six bias correction methods using observed and RCM data at upper Awash basin, Oromia, Ethiopia. *J. Water Clim. Change* **2022**, *13*, 664–683. [CrossRef]
78. Usman, M.; Manzanas, R.; Ndehedehe, C.E.; Ahmad, B.; Adeyeri, O.E.; Dudzai, C. On the Benefits of Bias Correction Techniques for Streamflow Simulation in Complex Terrain Catchments: A Case-Study for the Chitral River Basin in Pakistan. *Hydrology* **2022**, *9*, 188. [CrossRef]

Disclaimer/Publisher's Note: The statements, opinions and data contained in all publications are solely those of the individual author(s) and contributor(s) and not of MDPI and/or the editor(s). MDPI and/or the editor(s) disclaim responsibility for any injury to people or property resulting from any ideas, methods, instructions or products referred to in the content.